High Density Optical Memory using Photochromic Diarylethenes

辻岡, 強

https://doi.org/10.11501/3132442

出版情報：九州大学, 1997, 博士（工学）, 論文博士
バージョン：
権利関係：

High Density Optical Memory using Photochromic Diarylethenes

Tsuyoshi Tsujioka

High Density Optical Memory using Photochromic Diarylethenes

Tsuyoshi Tsujioka

1997

CONTENTS

CHAPTER 1

GENERAL INTRODUCTION

1.1 Brief History of Information Storage

The most significant development in optical data storage occurred 5000 years ago, when the Egyptians invented alphabetic and hieroglyphic writing. True writing systems, as opposed to drawings or pictograms, are essentially methods for the digital transmission of language information. A written description can convey a very precise understanding of an idea. Except for misspellings, the message can be copied many times without any loss of meaning - witness the remarkable preservation of ancient records through generations of handwritten manuscripts.

Figure 1-1 illustrates some of the dramatic developments in information storage that were motivated by the need for more convenient access and more efficient storage. The technological evolution depicted has been both a consequence and a cause of the rapidly increasing production of information. As the information age, the search for new storage technology, many of the resulting inventions reemphasized the importance of light and optics for information storage and communications.

In current usage, optical data storage refers to systems that use light to record as well as to reproduce information. Photography is the earliest example of optical recording. Silver-halide photography, which was developed over the last 200 years, has demonstrated remarkable achievements in analog image recording. Recent developments in electrophotography and holography have further extended our ability to record analog images and text rapidly, cheaply and compactly. However, the utility of analog images for information storage is limited. Digital computers, the centerpiece of information systems, require electronic and digital inputs. A considerable amount of processing is required to convert any analog signal into a machine-readable form. It is advantageous to convert information into a digital data stream.

Photography can be adapted for digital data recording. A number of high-speed, film-based data recorders, such as RCA system, have been built [1]. In these systems, a laser beam is modulated by the data signal as it scans rapidly and repetitively across a reel of films. Data rates of 20 Mbps and storage densities of 10^4 bit/mm^2 have been

demonstrated. However, these photographic film systems are limited to special applications, because the "tape" format inhibits rapid data access and because post-processing, either chemical or thermal, is necessary.

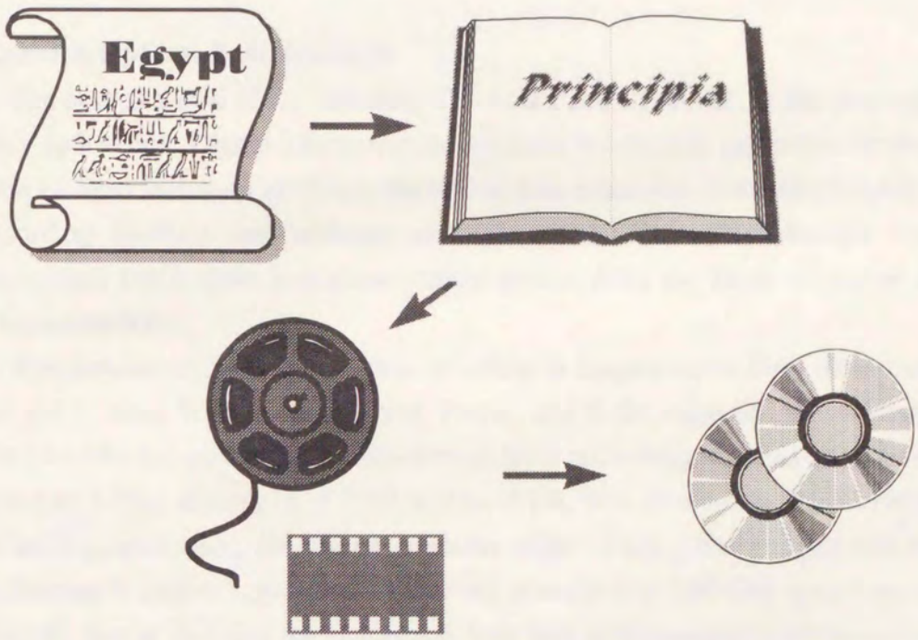

Figure 1-1. Evolution of optical data storage

The modern concept of optical recording, in which a light beam is used as a multi-purpose tool for writing and reading information, is based on the development of lasers. The concept of pulsing the beam to create discrete and micron-sized marks followed shortly. In fact such proposal was realized for the first time by using thin films of MnBi; this demonstration for magnetooptical recording corresponds quite closely with current systems. Maydan demonstrated the "micro-machining" of small holes in metal films and described the basic optical and thermal characteristics of the optical spot [2]. This work was the foundation for modern write-once optical recording.

1.2 Current Optical Data Storage

The compact disk (CD), including CD-Audio and CD-ROM, is the prototypical read-only optical disk. Digital information is replicated into the disk and cannot be altered. The most obvious limitation of CDs is the lack of data erasability. Erasability implies that the recording medium can undergo an unlimited number of write/erase cycles. Magnetooptical (MO) disks and phase-change optical disks are kinds of optical disks which have erasability.

The concept of high-density data recording in magnetooptic films dates back at least to 1957, when Williams, Sherwood, Foster, and Kelly suggested that a magnetic memory could be designed using a MnBi storage layer and a magnetic readout system [3]. The idea was further elaborated in 1958 by Mayer [4], who demonstrated that recording can be accomplished using the thermo-magnetic effect (Curie-point writing) and that a beam-addressable system is possible. The writing process of an MO disk is carried out by a heat-mode, that is, focusing the high power laser light to the magneto-optical recording layer, increasing the temperature and changing the magnetization locally, usually with an external bias field. Figure 1-2 illustrates how the magnetooptic Kerr effect can be used to sense vertical magnetic domains. In this situation, the polarization rotation is called the polar Kerr effect. The sense of rotation depends on whether the magnetization is aligned parallel to or opposite to the incident light direction. A focused beam can be used to sense the magnetization in a small spot.

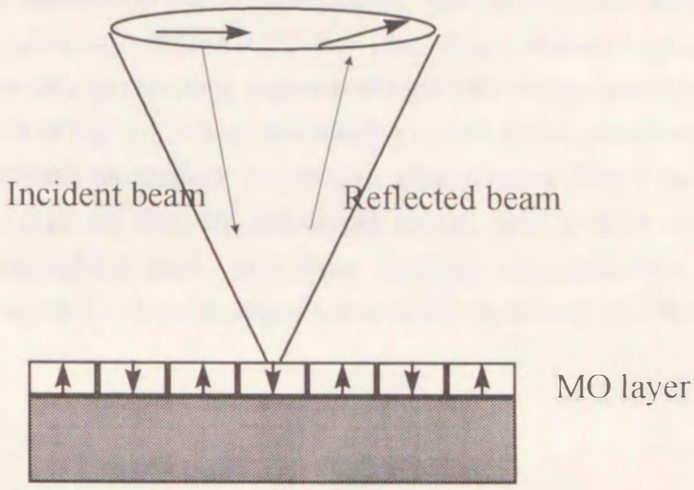

Figure 1-2. MO readout. The Kerr effect can be used to sense perpendicular magnetic domain.

The most promising alternative to magneto-optics for erasable optical recording is phase-change recording. Many materials can exist in several different crystalline phases. Although only one phase is energetically favored, alternate structures can exist in local minima. The meta-stable state can be switched to the stable state by applying a considerable large activation energy. The switching can be accomplished by appropriate thermal heating. If the temperature is low enough, the new structure is essentially permanent. Ovshinsky described how amorphous/crystalline phase switching can be used for optical data storage [5]. He demonstrated such switching behavior in a variety of semiconductor-based materials, especially chalcogenides (glasses based on the chalcogen elements S, Se and Te). The typical phase-change optical recording material is a multi-component alloy that has a stable, crystalline phase and a meta-stable amorphous phase with different optical properties. In an erasable phase-change system, annealing is the technique for erasure; the erase beam heats the data track to a temperature just below the melting point long enough to recrystallize and erase any amorphous marks. Recording is accomplished by locally melting the recording material using light energy and then cooling it quickly enough to quench it in the amorphous phase. Readout is carried out by

detecting the reflectance change between the crystalline phase and amorphous phase.

If phase-change materials could be optimized for both rapid erasure and reliable recording, a simple single-beam method for overwriting with a standard optical head could be realized. Phase-change recording materials designed for this purpose have been developed [6]. As shown in Fig. 1-3, complete annealing occurs during one scan past the optical spot if the laser heats the medium to moderate a temperature. But if the laser is pulsed high enough to melt the film, the subsequent cooling time is short enough to partially quench the amorphous mark, preventing complete recrystallization. Phase-change systems can be applied to erasable digital versatile disk systems (DVD-RAM).

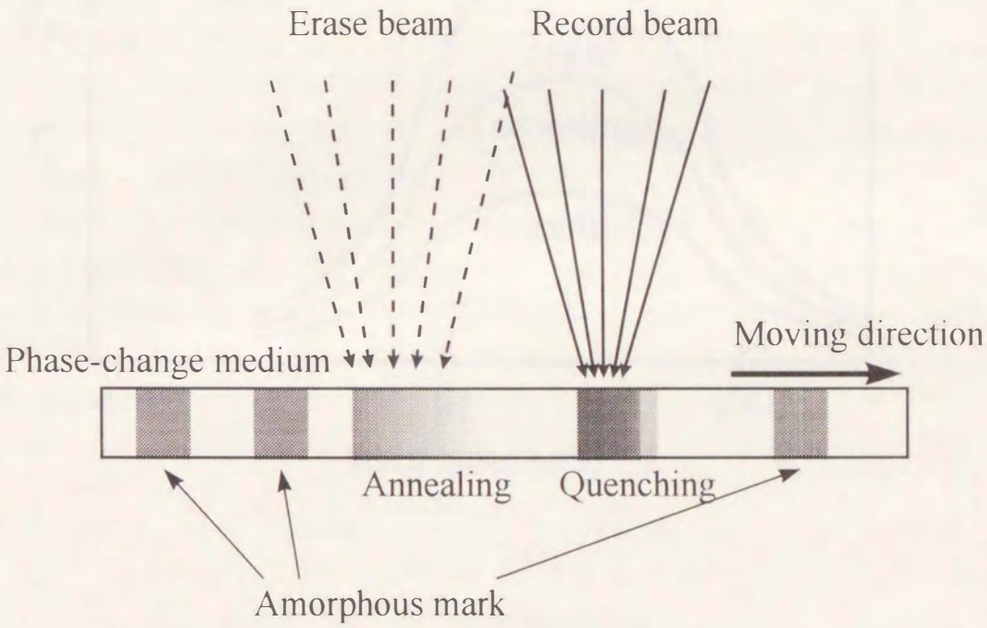

Figure 1-3. Writing and erasure of a phase-change medium.

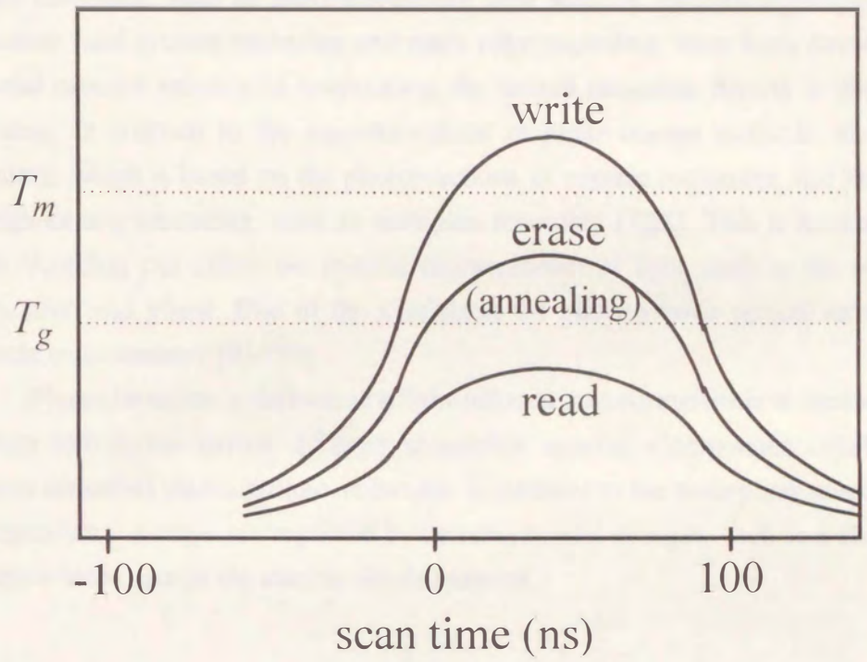

Figure 1-4. Differential thermal cycles for single beam overwrite in a phase-change medium.

1.3 Photochromic Memory

MO and phase-change recording systems, which are based on the heat-mode reaction, are commercially available. In such systems, focused light energy is converted into heat energy on the recording medium. Recording density (or the recording mark-size) is limited by the size of the laser spot and, therefore, by the wavelength of the recording laser light. On the other hand, the demand for high-speed computing and large-data computation have been growing indefinitely and a variety of techniques for high-density recording, such as short-wavelength light sources, magnetically-induced super-resolution, land groove recording and mark edge recording, have been developed. The potential cardinal solution to overcoming the limited recording density is photon-mode recording. In contrast to the magneto-optical or phase-change methods, photon-mode recording, which is based on the photoreactions of organic molecules, has the potential for high-density recording, such as multiplex recording [7][8]. This is because photon-mode recording can utilize the specific characteristics of light, such as the wavelength, polarization and phase. One of the candidates for photon-mode optical recording is a photochromic memory [9]-[19].

Photochromism is defined as a light-induced transformation in a chemical species between two forms having different absorption spectra. Compounds capable of this reaction are called photochromic molecules. In addition to the absorption spectral change, isomerization is always accompanied by certain physical changes, such as a change in the refractive index and/or the electric dipole moment.

$$\mathrm{A} \underset{h\nu'}{\overset{h\nu}{\rightleftharpoons}} \mathrm{B}$$

The requirements that the photochromic memory should have are as follows:

1) Archival storage capability (thermal stability of both isomers).
2) Fatigue resistance (the cycle can be repeated many times without significant loss of performance).
3) Nondestructive readout capability.
4) Sensitivity at wavelengths of diode lasers or other light sources.
5) Suitable recording sensitivity.
6) Higher performance than conventional data storage systems.

The concept of wavelength-multiplexed (multi-wavelength) recording using

photochromic spiropyrans (Fig. 1-5) has been proposed [15]-[17][20]. Spiropyrans that have two long chains were found to be able to form stable Langmuir-Blodgett (LB) films. LB films, under UV irradiation at a temperature above 35℃, exhibited a sharp and intense band at a longer wavelength, which could be attributed to the formation of J-aggregates. The half-decay period in the dark was 10^4 times longer than that of conventional spiropyrans. The LB film containing different kinds of spiropyran J-aggregates was accumulated into a multi-layered recording medium, as shown in Fig. 1-5. Multi-wavelength recording using the medium was demonstrated (Fig. 1-6), but considerably large crosstalk between multiplexed channels was observed.

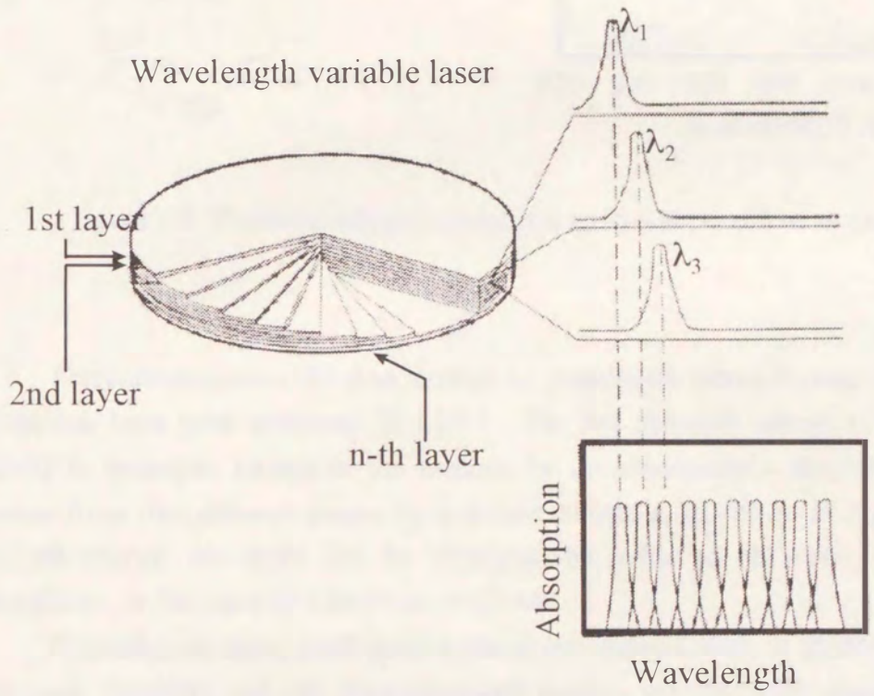

Figure 1-5. Concept of multi-wavelength recording.

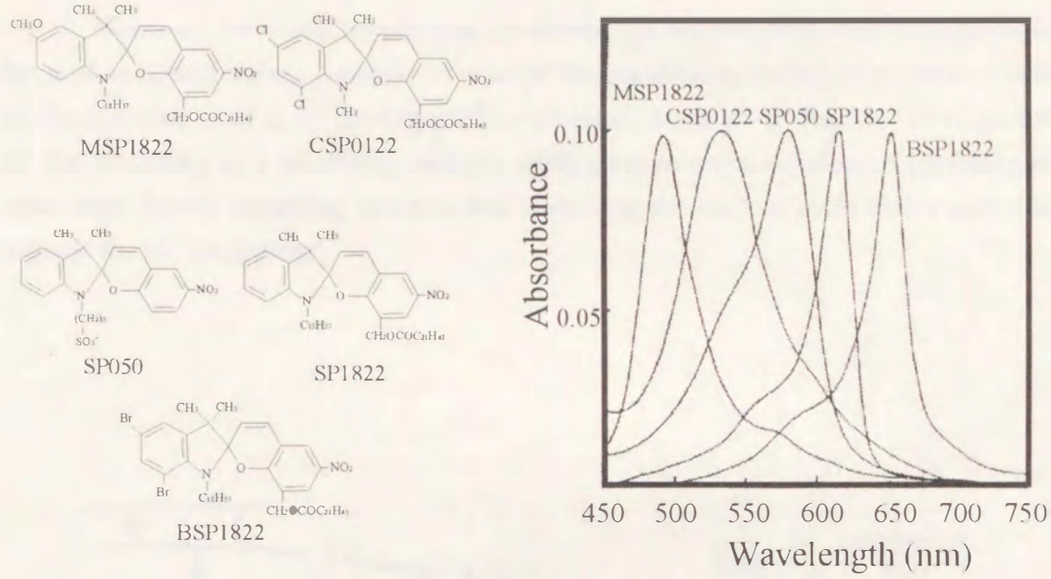

Figure 1-6. Photochromic spiropyrans for multi-wavelength recording.

Three-dimensional (3D) data storage by two-photon photochromic reactions of spiropyrans have been proposed [21]-[25]. The key principle behind a two-photon memory is molecular change in the medium by the simultaneous absorption of two photons from two different beams by a dopant molecule, as shown in Fig. 1-7. The localized change can store bits by changing the index of refraction, absorption, fluorescence, or the material's electrical properties.

Photochromic compounds used in the above systems, such as spirobenzopyrans, have poor durability and the photogenerated isomers are thermally unstable. These compounds can not be applied for practical use. Recently, a new type of photochromic compounds, which have thermally irreversible and fatigue resistance properties, have been developed [26][27]: diarylethenes with heterocyclic rings, such as 1,2-bis-(2-methylbenzo[b]thiophen-3-yl) perfluoro-cyclopentene **(1)**, and 2-(1,2-dimethyl-3-indolyl)-3-(2,4,5-trimethyl-3-thienyl) maleic anhydride **(2)** (Fig. 1-7). These compounds have no thermochromicity even at 300℃ and their colored closed-ring forms are stable for more than three months at 80℃. Furthermore, the cycle of ring-closure/ring-opening can be repeated more than 10^4 times with keeping the photochromic performance. Thus, diarylethene derivatives are among the most promising photochromic compounds for

high-density optical memory media.

However, there still remain many problems for the photochromic compounds to be used as optical memory media. To solve these problems, recording systems as well as the materials need to be developed. The necessary items are as follows: investigation on the sensitivity as a recording medium, application to multi-wavelength recording or other high-density recording systems, and improving the readout cycle ability and light sources for photoreactions.

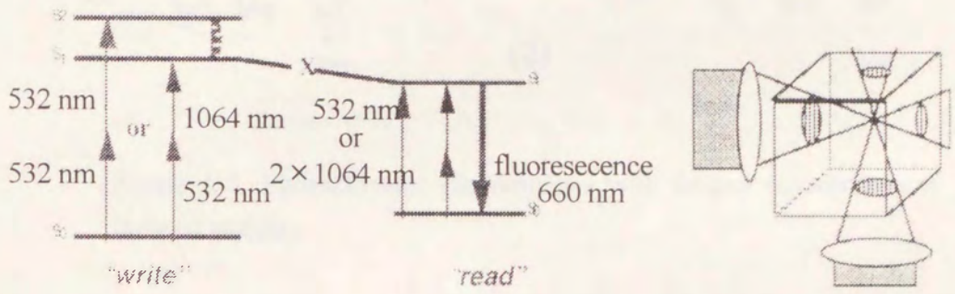

Figure 1-7. 2-photon data storage

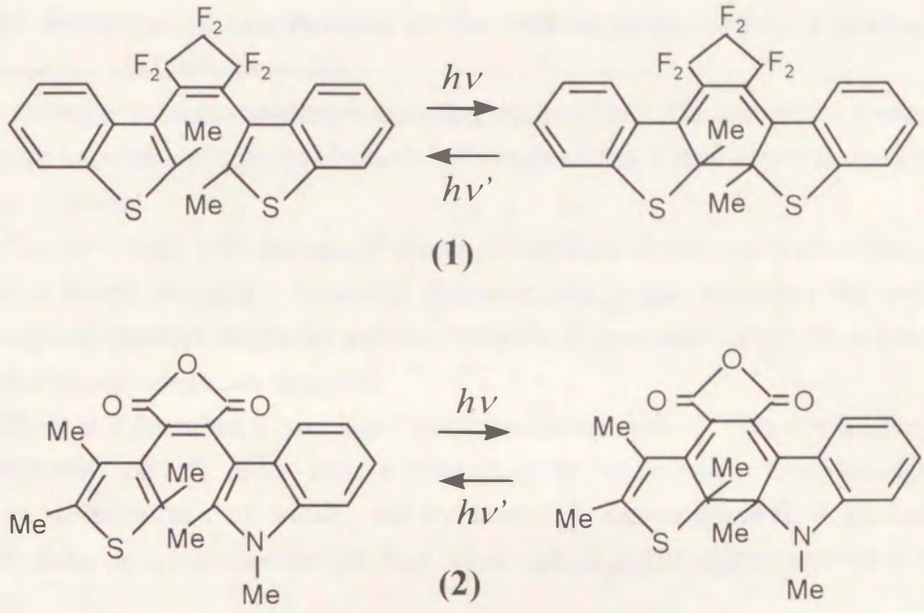

Figure 1-8. Photochromic diarylethenes with fatigue resistance and thermal stability.

1.4 Objectives of this study

This thesis deals with results obtained from research on the application of photochromic diarylethenes to high-density optical memory media. To gain access to the optimum molecular design of photochromic compounds, various requirements for optical memory systems were examined and simulated, and some new concepts of writing/reading method are proposed. The notations used in this study are summarized in Table 1-I.

In chapter 2, light sources for photochromic reactions are described. Coloring and bleaching reactions of photochromic diarylethenes are performed using a single GaN-based LED.

Chapter 3 describes the photochromic reaction of a diarylethene derivative in polymer matrices. Energy transfer from an open-ring to a closed-ring form is suggested as a possible mechanism for the time dependence of the sensitivity in the polymer film containing a high chromophore concentration.

Chapter 4 examines the quantitative relation between the sensitivity of

photochromic compounds and the possible data transfer rate of an optical memory. To avoid the destruction of data recorded on the medium during reading, a method of superlow-power readout is proposed.

In chapter 5, multi-wavelength recording are described. The theoretical treatment of crosstalk between multiplexed channels is formulated and a new crosstalk reduction method is proposed.

Chapter 6 deals with the optical density dependence of write/read characteristics in a photochromic memory. Improved characteristics in the secondary harmonics, superlow-power readout properties and the crosstalk of multi-wavelength recording for high optical density media are examined.

Chapter 7 describes a new high-density recording method. This is a method of super-resolution optical disks with a photochromic mask layer. Super-resolution properties are analyzed theoretically, and the method is demonstrated for high-density read-only disks. A super-resolution method for an optical disk mastering method is also analyzed.

Chapter 8 gives a general conclusion reached as a result of this study.

Table 1-I Parameters and constants used in our analysis and estimates.

parameter	unit	meaning
C	M (mol/l)	concentration of chromophore
C_X	M	concentration of chromophore X
ε	$M^{-1}cm^{-1}$	molar extinction coefficient
ε_{Xi}	$M^{-1}cm^{-1}$	molar extinction coefficient(of molecule X at λ_i
ϕ		photoreaction quantum yield
ϕ_{Xi}		photoreaction quantum yield of molecule X at λ_i
λ	m	wavelength of light
λ_i	m	wavelength of i-th light
t	s	time
t_W	s	irradiated light pulse width
X	m	coordinate fixed on the medium (tangential direction)
Y	m	coordinate fixed on the medium (radial direction)
n		number of absorbed photon
n_{Xi}		number of absorbed photon with wavelength λ_i by molecule X
N		number of reacted molecule
N_X		number of reacted molecule X
Abs		Absorbance
Apt		Absorptance
R		reflectance of the medium
R_{rec}		reflectance of the recording layer
R_{ref}		reflectance of the reflective layer
R_{ini}		reflectance in the initial state
R_{mark}		reflectance in the recorded mark
ΔR		change in reflectance (R_{mark}-R_{ini})
T		transmittance of the layer including chromophore
T_0		initial transmittance of the layer including chromophore
OD		optical density of the layer including chromophore

S	cm^2	light irradiation area
P	W	light intensity
P_i	W	light intensity of i-th wavelength λ_i
P_{rep}	W	readout light intensity
v	m/s	relative speed between a spot and a memory medium
L	cm	thickness of the layer including chromophore
γ		pickup efficiency (ratio of light intensity arriving at the photodiode and reflected from the medium)
η	A/W	photoelectric conversion efficiency of the photodiode at unity gain
I	A	photocurrent
B	Hz	system band width
$\mathbf{R_b}$	bps	data transfer rate
SNR		signal-to-noise power ratio
SNR_0		signal-to-noise power ratio required for the system
h	Js	Plank's constant (6.626×10^{-34})
c	m/s	light speed in vacuum (3.00×10^{8})
e	C	elementary charge (1.602×10^{-19})
N_a	mol^{-1}	Avogadoro's number (6.02×10^{23})
α	mol/Jm	a constant defined by $2.303 \times 10^{3}/N_a hc = 1.92 \times 10^{4}$

CHAPTER 2

Light Source for Photochromic Devices (GaN based Light Emitting Diode)

2.1 Introduction

Interest in developing and using organic photochromic compounds for optical memory media, photooptical switches and other photonic devices has been growing.[14][18][26][28]-[38] A new type of photochromic compound which has thermally irreversible and fatigue resistance properties has been developed by M. Irie et.al.[14][26] The compounds are diarylethenes with heterocyclic rings, such as 2-(1,2-dimethyl-3-indolyl)-3-(methylbenzo[b] thiophen-3-yl) perfluorocyclopentene **(1)**, and 1,2-bis-(2-methylbenzo [b]thiophen-3-yl) maleic anhydride **(2)**.

When we apply the compounds to optical memory media, a serious technological problem remains unsolved. A reversible photochromic reaction requires two light beams of different wavelength, one for coloring and one for bleaching. For example, a bleaching reaction can be carried out using a laser diode or a light-emitting diode with a wavelength in the visible range. However, many compounds require ultraviolet (UV) light for the coloring process. Various UV light sources, such as Hg lamps or HeCd-gas lasers, have been used. However, in practical applications, smaller and lower-cost light sources, such as laser diodes or light-emitting diodes (LED), are desirable. The ideal light source is a single laser diodes or LED's, which can induce both coloring and bleaching processes. Recently, high-intensity blue/green light-emitting diodes having a GaN-based active layer have been developed.[39][40] It is expected that such LEDs can be used in photochromic devices.

In this chapter, the feasibility of performing photochromic reactions using a single GaN-based LED is investigated.

2.2. Results

We used two species of photochromic diarylethenes in toluene solution: hexafluorocyclopentene diarylethene **(1)** and maleic anhydride diarylethene **(2)**. The open-ring state **(1a)** of diarylethene **(1)** converts to the closed-ring state **(1b)** by irradiation with ultraviolet light and the absorption in the visible-wavelength region (400-700 nm) increases. On the other hand, the closed-ring state **(1b)** converts to the open-ring state **(1a)** by irradiation with visible light and the absorption in this wavelength region decreases. The open ring state **(2a)** of diarylethene **(2)** converts to the closed ring state **(2b)** by irradiation with blue-green light, and the absorption in the green wavelength region (500-600 nm) increases. Conversely, the closed-ring state **(2b)** converts to the open ring state **(2a)** by irradiation with green light and the absorption in the green wavelength region decreases.

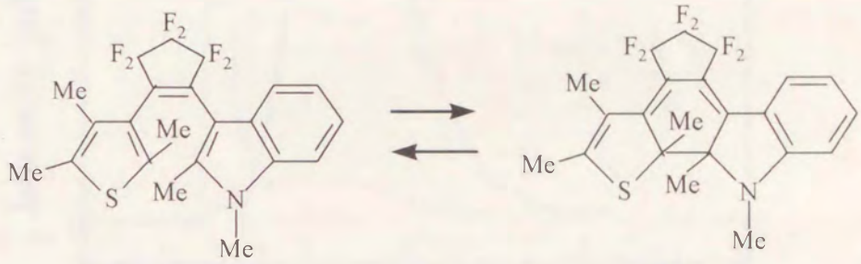

(1a) **(1b)**

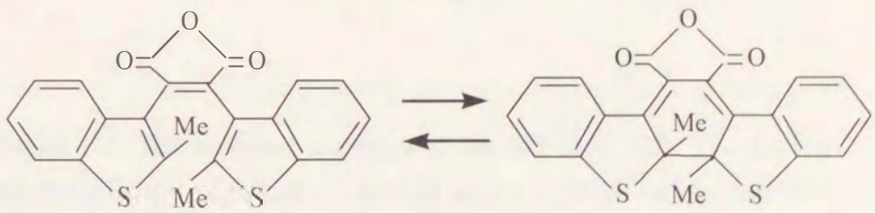

(2a) **(2b)**

We used GaN-based light emitting diodes as the light source for these photo-reactions. The diodes consist of a double hetero-structure (DH) (blue LED: Nichia, NLPB500) or a single-quantum well structure (SQW) (green LED: Nichia, NSPG300A). These LEDs emit light of different wavelengths depending on the type of drive current.

Figure 2-1 shows the luminous spectrum of the DH blue LED. With constant current, the LED emits blue light with a broad peak at a wavelength of approximately 450

nm. However, when driven by large pulsed current, the LED emits high-intensity ultraviolet light with a sharp peak at a wavelength of 380 nm. Therefore, ultraviolet light generated by the LED driven by pulsed current can be used for the ring-closure reaction, and blue light generated by the LED driven by constant current can be used for the ring-opening reaction of diarylethene **(1)**.

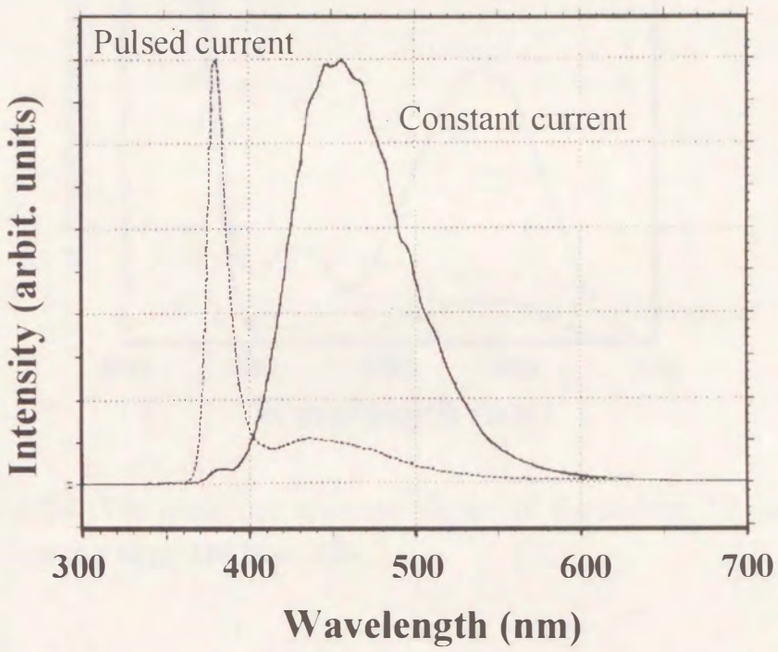

Figure 2-1. The luminous spectrum of the DH blue LED. The driving conditions were as follows. The peak value of the pulsed current was 400 mA, the duty ratio was 1/20, the frequency was 20 kHz and peak emitted power was about 10 mW. The value of the constant current was 20 mW and the emitted power was about 1 mW.

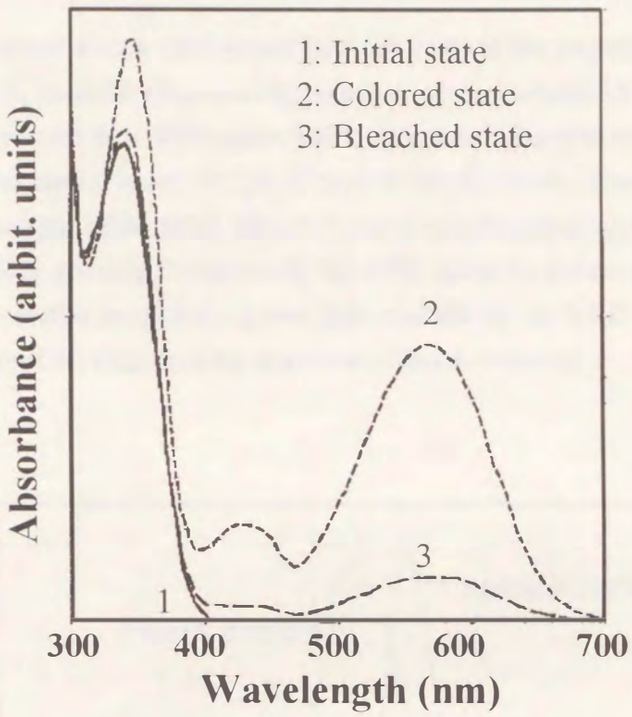

Figure 2-2. The absorption spectrum change of diarylethene **(1)** upon exposure to a single DH blue LED.

Figure 2-2 shows the absorption spectral change of diarylethene **(1)** upon exposure to the DH blue LED. The initial state was a purely open-ring state with no absorption at wavelengths in the visible range. Upon irradiation with ultraviolet light of the DH blue LED driven by pulsed current, the ring-closure (coloring) reaction occurred. The absorption in the visible light region increased. (The isomerization ratio was about 0.5.) A peak value of the pulsed current of 400 mA, a duty ratio of 1/20, a frequency of 20 kHz and a peak emitted power of about 10 mW were employed.

The ring-opening (bleaching) reaction was induced due to irradiation with blue light from the DH LED driven by constant current. In this case, the value of the current was 20 mA and the emitted power was about 1 mW. The small amount of absorption remaining is due to weak emission of ultraviolet light (Fig. 2-1).

It can be seen from these results that the photochromic coloring and bleaching reactions of diarylhexafluorocyclopentenes were carried out using a single GaN-based

DH LED.

As mentioned above, blue-green light can be used for ring-closure reactions and green light can be used for ring-opening reactions of diarylethene **(2)**. Figure 2-3 shows the luminous spectrum of a SQW green LED. At constant current, the LED emits green light with a broad peak at a wavelength of approximately 530 nm. Employing large pulsed current, this broad peak of emitted light shifted to a wavelength of approximately 500 nm. Therefore, the blue-green light emitted by the LED driven by pulsed current can be used for ring-closure reactions, and the green light emitted by the LED driven by constant current can be used for ring-opening reactions of diarylethene **(2)**.

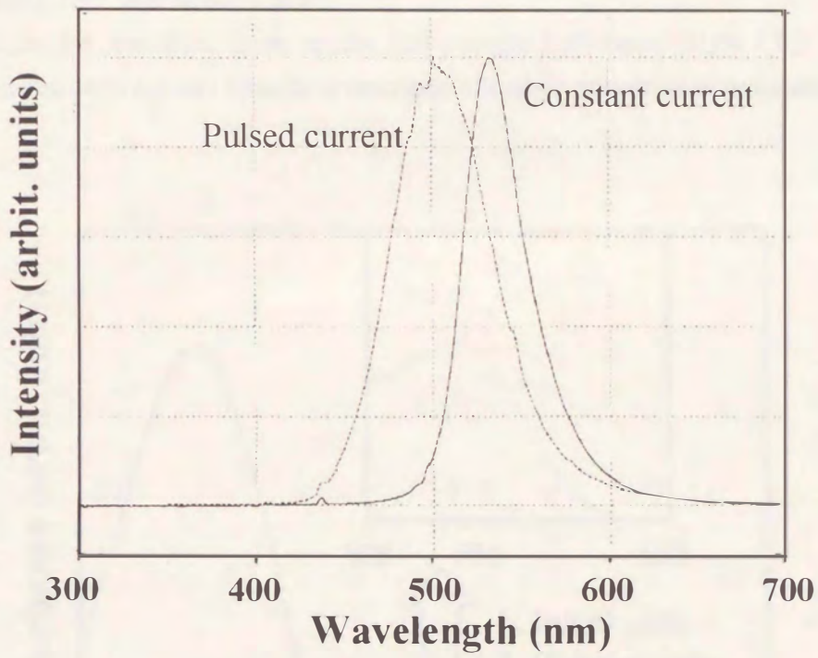

Figure 2-3. The luminous spectrum of a SQW green LED. The peak value of the pulsed current was 400 mA, the duty ratio was 1/20, the frequency was 20 kHz and the peak emitted power was about 12 mW. The constant current was 20 mA and emitted power was about 1 mW.

Figure 2-4 shows the absorption-spectrum change of diarylethene **(2)** upon exposure to the SQW green LED. The initial state was a purely open-ring state with no absorption in the wavelength region of 500-600nm. Upon irradiation with blue-green light of the SQW LED driven by pulsed current, the ring-closure (coloring) reaction occurred. The absorption in the wavelength region of 500-600nm increased. A peak value of the pulsed current of 400 mA, a duty ratio of 1/20, a frequency of 20 kHz and a peak emitted power of about 12 mW were employed. The isomerization ratio was low (about 0.06) because the light included a green wavelength component, which induces the reverse (bleaching) reaction simultaneously.

The ring-opening (bleaching) reaction was induced by irradiation with green light of the SQW LED driven by a constant current. In this case, the current was 20 mA and the emitted power was about 1 mW.

It can be seen from these results that a single GaN-based SQW LED can induce photochromic coloring and bleaching reactions of maleic anhydride diarylethene.

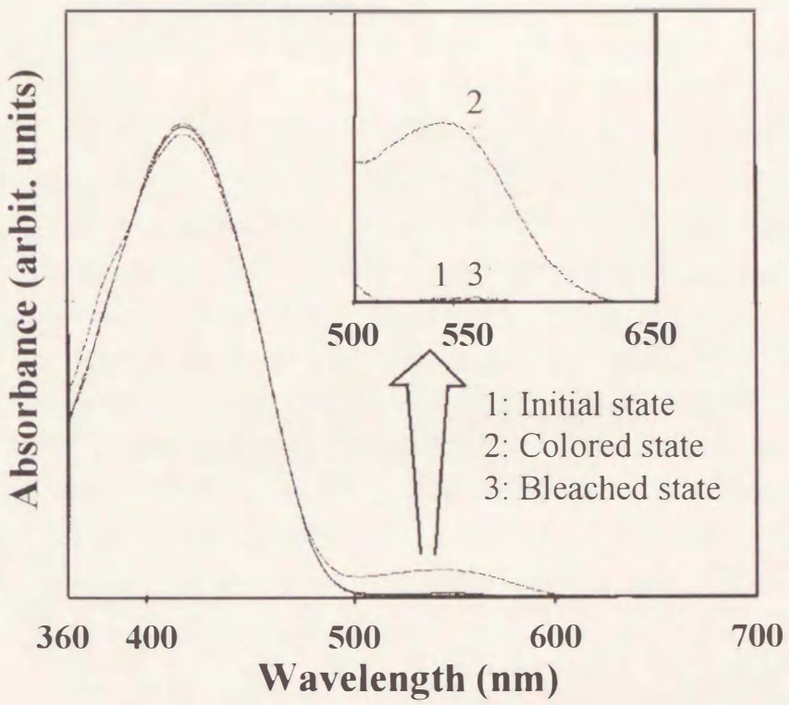

Figure 2-4. The absorption spectrum change of diarylethene **(2)** upon exposure to a single SQW green LED.

2.3. Conclusion

The photochromic coloring and bleaching reactions for photochromic diarylethenes were performed using a single GaN-based LED. GaN-based light-emitting devices are promising light sources for photochromic devices.

CHAPTER 3

Photochromic Reactivity of a Diarylethene Derivative in Polymer Matrices

3.1 Introduction

Interest in developing and using organic photochromic compounds for rewritable optical memory media has been growing.[14][18][25][26][33]-[36][40]-[50] Indispensable properties that these compounds should have include thermal stability of both isomers and high resistance to thermal and photochemical degradation. A new type of photochromic compounds which have thermally irreversible and fatigue resistance properties has been developed.[14][26][34][35] The compounds are diarylethenes with heterocyclic rings, such as 1,2-bis-(2-methylbenzo[b] thiophen-3-yl) perfluorocyclopentene,[35] and 2-(1,2-dimethyl-3-indolyl)-3-(2,4,5-trimethyl-3-thienyl) maleic anhydride **(1a)**.

These compounds have no thermochromicity even at 300℃ and their colored closed-ring forms are stable for more than 3 months at 80℃.[14] Furthermore, the cycle of ring-closure/ring-opening can be repeated more than 10^4 times with keeping the photochromic performance.[14][34] Thus, diarylethene derivatives are among the most promising photochromic compounds for rewritable optical memory media.

In general, solid-state thin films containing a photochromic compound are used for photochromic memory media. When photochromic compounds are dispersed in solid polymer matrices, the reactivities are changed from those in a homogeneous solution. For example, the thermal reverse processes no longer follow the 1st-order kinetics.[48]-[58] In this study, we investigated the photochromic reaction of **(1a)** in poly(vinyl butyral) and found that sensitivity depends on both concentration and irradiation light wavelength.

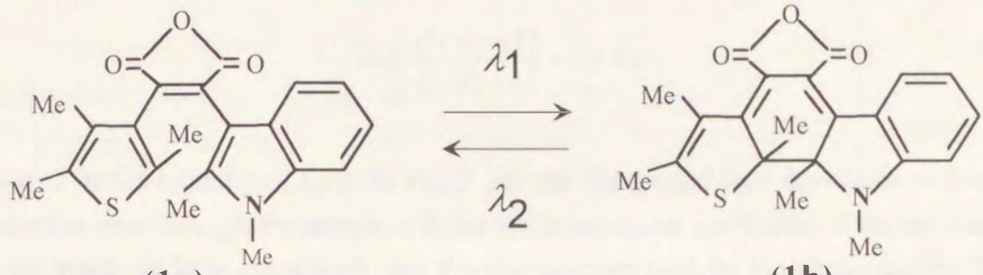

(1a) **(1b)**

3.2 A Model of a Photochromic Reaction

The following equation has been frequently used to measure the photochemical quantum yield,[55] [56]

$$\log\left(\frac{P / P_0 - 1}{P / P_t - 1}\right) = \varepsilon \phi P t \qquad (3\text{-}1)$$

where P is the intensity of light, P_0 and P_t are the transmitted light intensities at times 0 and t that pass through the sample, ε is the molar extinction coefficient of the compound at the irradiated light wavelength, and ϕ is the quantum yield for the photoreaction. This equation was derived under the following conditions.

(i) Light is absorbed only by the reactant molecule, and not absorbed by the product molecule. The reverse photoreaction is ignored.
(ii) The photoreaction is of the 1st order. (i.e. a molecule reacts with a unique sensitivity by absorbing a photon.)
(iii) Light for the photoreaction is monochromatic.
(iv) Light absorption by the medium and decomposition of the compounds are negligible.

We can obtain a straight line for the photoreaction by plotting the left-hand side of eq. (3-1) with time, and derive a unique quantum yield from the inclination.

In order to treat the generalized process, such as a coloration process of diarylethenes, we modified the above first condition as follows.

(i) Light is absorbed by both the reactant and product molecules. The reverse photoreaction is also taken into account.

Furthermore, for simplicity, we assumed the additional condition that the absorbance (Abs) of the sample at the irradiation wavelength is low. ($Abs \leq 0.2$) Under these conditions, we derived a generalized equation for the photochromic reactions.

We consider the case that both the reactant isomer **(a)** (open-ring form) and the product isomer **(b)** (closed-ring form) have absorption (molar extinction coefficients ε_a and ε_b) at the irradiation wavelength and are able to react (quantum yields ϕ_a and ϕ_b). Isomer **(a)** and **(b)** change each other by photoirradiation. Absorptance (Apt) at wavelength λ is

$$Apt = 1 - \exp(-2.303Abs) = 1 - \exp\left(-2.303\left(\varepsilon_a C_a + \varepsilon_b C_b\right)L\right)$$
$$\approx 2.303\left(\varepsilon_a C_a + \varepsilon_b C_b\right)L \qquad (3\text{-}2)$$

where C_a and C_b are the concentrations of isomers **(a)** and **(b)**, respectively, and L is sample thickness. The low absorbance approximation was used in eq. (3-2). The photochromic reaction can be treated to proceed homogeneously in the approximation.

Following differential equation is derived by considering the relation between absorbed photons and reacting molecules.

$$\frac{\partial C_b}{\partial t} = \alpha \frac{P\lambda}{S}\left(\varepsilon_a \phi_a + \varepsilon_b \phi_b\right)\left[C_b - \frac{\varepsilon_a \phi_a}{\varepsilon_a \phi_a + \varepsilon_b \phi_b} C_0\right] \qquad (3\text{-}3)$$

where C_0 is total concentration (C_a+C_b). Equation (3-3) is easily integrated and we obtain an equation that is directly applicable to experimental measurements,

$$-\ln\left(\frac{Abs(t) - Abs(\infty)}{Abs(0) - Abs(\infty)}\right) = \alpha \frac{P\lambda}{S}\left(\varepsilon_a \phi_a + \varepsilon_b \phi_b\right)t, \qquad (3\text{-}4)$$

where $Abs(t)$ indicates the absorbance at wavelength region λ_2 at time t. Note that eq. (3-4) can be applied to both coloring and bleaching processes. When the photoreaction follows 1st-order kinetics, we can obtain a linear time dependence by plotting the left-hand side quantities, and the unique value for the total sensitivity $\varepsilon_a\phi_a+\varepsilon_b\phi_b$ is deduced. On the other hand, for non-1st-order reactions, the plotting will be curved and a unique value for the sensitivity cannot be obtained. In order to analyze such nonlinear time dependence, we derived eq. (3-5) from eq. (3-4),

$$-\ln\left(\frac{Abs(t + \Delta t) - Abs(\infty)}{Abs(t) - Abs(\infty)}\right) = \alpha \frac{P\lambda}{S}\left(\varepsilon_a \phi_a + \varepsilon_b \phi_b\right)\Delta t \qquad (3\text{-}5)$$

where Δt indicates the measuring time interval. The sensitivity obtained by eq. (3-5) corresponds to the differential coefficient at time t of the plotting with left-hand side of eq. (3-4).

3.3 Experimental

We prepared three kinds of samples: benzene solution containing **(1)** (4.0×10^{-5} M), poly(vinyl butyral) (PVB) films containing a low concentration of **(1)** (0.036 M; film thickness, 12 μm), and PVB films containing a high concentration of **(1)** (1.0 M; film thickness, 0.4 μm). The thickness of each sample was calibrated such that the absorbance is identical each other and the low absorbance condition ($Abs \leq 0.2$) is satisfied at the wavelength of light for photo-reaction. Usually, one can get the sensitivity by measuring the absorbance change in the coloring process; although, it was difficult to follow the coloring process because of a rather low conversion in the polymer film. Therefore, we prepared colored film samples by spin-coating with the cyclohexanone solution containing colored closed-ring forms of **(1b)** and PVB on the glass substrates, and the absorbance change in the bleaching process was followed. No micro-crystals in the samples were observed using a polarizing microscope and therefore the photochromic molecules were dispersed homogeneously in the polymer matrices.

We adopted an Ar ion laser and a HeNe laser as light sources (200 $\mu W/cm^2$). 477nm light was used for coloring, and 515nm and 633nm lights were used for bleaching. The absorbance of the samples was measured with a multipurpose recording spectrophotometer (Shimadzu, MPS-2000).

3.4 Results and Discussion

Figure 3-1 shows the absorption spectral change of **(1)** in a benzene solution. Upon irradiation with 477nm light, a new peak appeared at 600nm. The new peak was bleached by irradiating with 515nm or 633nm light. The coloration/decoloration cycles can be repeated many times.

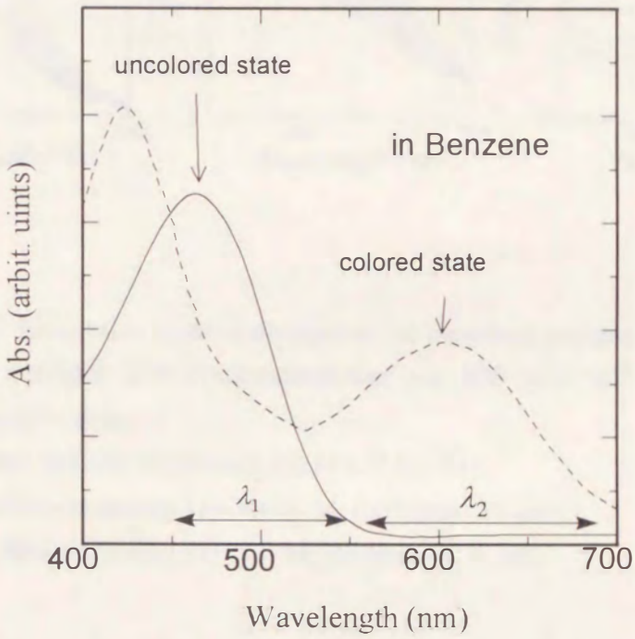

Figure 3-1 Absorption spectral change of diarylethene **(1)** in the benzene solution (4.0×10^{-5} M) by irradiation with 477 nm light.

Figure 3-2 shows the spectral changes induced by irradiation with 515nm light, which can excite both isomers. The absorbance of the closed-ring forms in benzene solution and in the polymer film containing a low chromophore concentration decreased with irradiation time and tended to level off. On the other hand, the bleaching rate in the film containing a high concentration was much larger. This indicates that the reaction mechanism depends on the concentration of the chromophore in the polymer film.

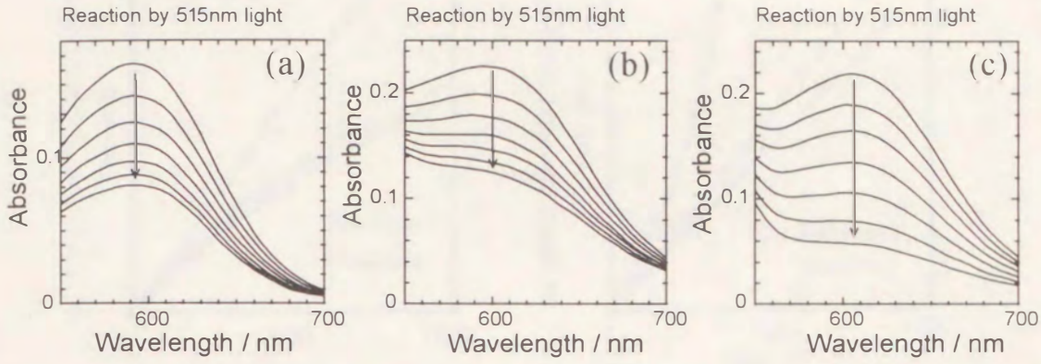

Figure 3-2 Absorption spectral changes in the bleaching process by irradiation with 515 nm light. The irradiation power was 200 μ W/cm^2 and the time interval was 30 s/line.

(a) benzene solution containing **(1)** (4.0×10^{-5} M).

(b) PVB film containing **(1)** (0.036 M; thickness, 12 μm).

(c) PVB film containing **(1)** (1.0 M; thickness, 0.4 μm).

Figure 3-3 shows the irradiation time dependence of the left-hand side of eq. (3-4) for the bleaching process. The time dependence for the bleaching process by irradiating with 633nm light is also shown. (Note that only the closed-ring forms are excited with 633 nm light.) The bleaching process in the benzene solution followed the 1st-order kinetics, while in polymer film the bleaching processes deviated from the 1st-order kinetics. When 515nm light was used, the bleaching processes in benzene solution and in the low concentration film obeyed the 1st-order kinetics, while the plots for the high concentration sample strongly deviated from the 1st-order kinetics. The deviation tendency was dependent on the irradiation wavelengths of 515nm and 633nm.

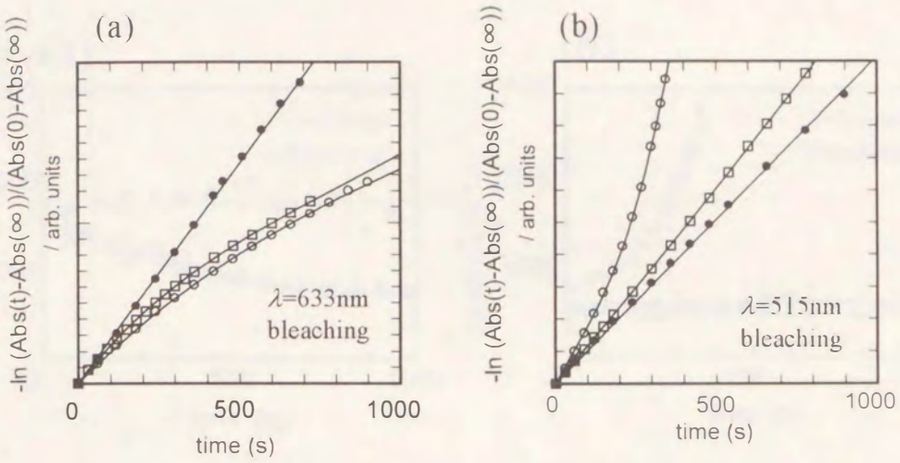

Figure 3-3. Irradiation time dependence of the left-hand side of eq. (3-4). Only the closed-ring form was excited with 633nm light (a), while both isomers were excited with 515nm light (b).

○; PVB sample (1.0 M; thickness, 0.4 μm).

□; PVB sample (0.036 M; thickness, 12 μm).

●; benzene solution (4.0×10^{-5} M).

Figures 3-4 **(a)** and **(b)** show the irradiation time dependence of the sensitivity ($\varepsilon_a\phi_a+\varepsilon_b\phi_b$), derived by using eq. (3-5). When the samples were irradiated with 633nm light, they gradually decreased in the polymer film. In the benzene solution, they were constant. When irradiated with 515nm light, the sensitivity of the high concentration film dramatically increased. This indicates that the ring-opening reaction sensitivity dramatically increases with time.

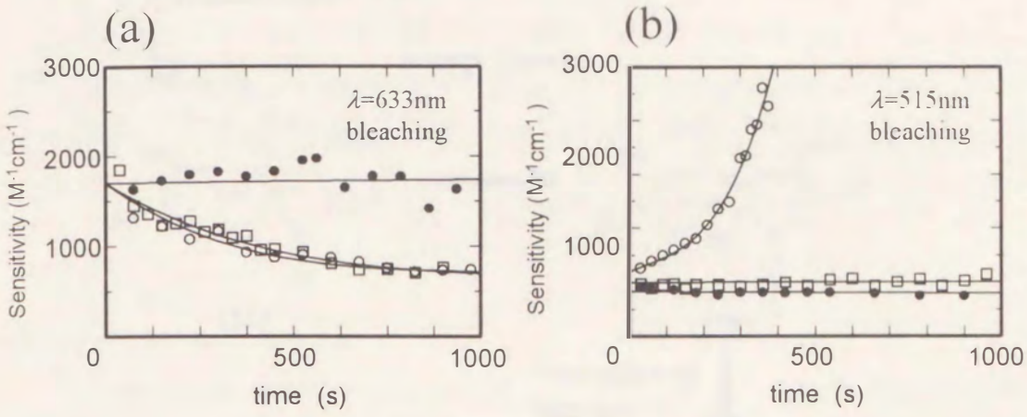

Figure 3-4. Irradiation time dependence of the sensitivity $\varepsilon_a\phi_a+\varepsilon_b\phi_b$. These sensitivities were determined by using eq.(3-5).

○; PVB sample (1.0 M; thickness, 0.4; thickness,0.4 μm).

□; PVB sample (0.036 M; thickness, 12 μm).

●; benzene solution (4.0×10^{-5} M).

The total sensitivity increased to 5 times as much that of the initial sensitivity. In terms of the expression of total sensitivity $\varepsilon_a\phi_a+\varepsilon_b\phi_b$ and the low conversion ratio, this increase indicates that the ring-opening sensitivity $\varepsilon_b\phi_b$ increased. The initial quantum yield ϕ_b was 0.4, while it increased to 2.0. Such a large increase in the quantum yield indicates the contribution of an additional bleaching process through an energy transfer. The photoexcited open-ring form transfers its energy to a neighboring closed-ring form, and the closed-ring molecule is transformed to the open-ring form.

Figure 3-5 schematically shows the reaction mechanism. When light is absorbed only by the closed-ring form, a normal ring-opening reaction occurs. On the other hand, when light is absorbed by both isomers, an additional ring-opening reaction due to energy transfer takes place when the concentration of the open-ring form is high. As a result, the ring-opening reaction sensitivity becomes large and the conversion ratio from open-ring form to closed-ring form is suppressed.

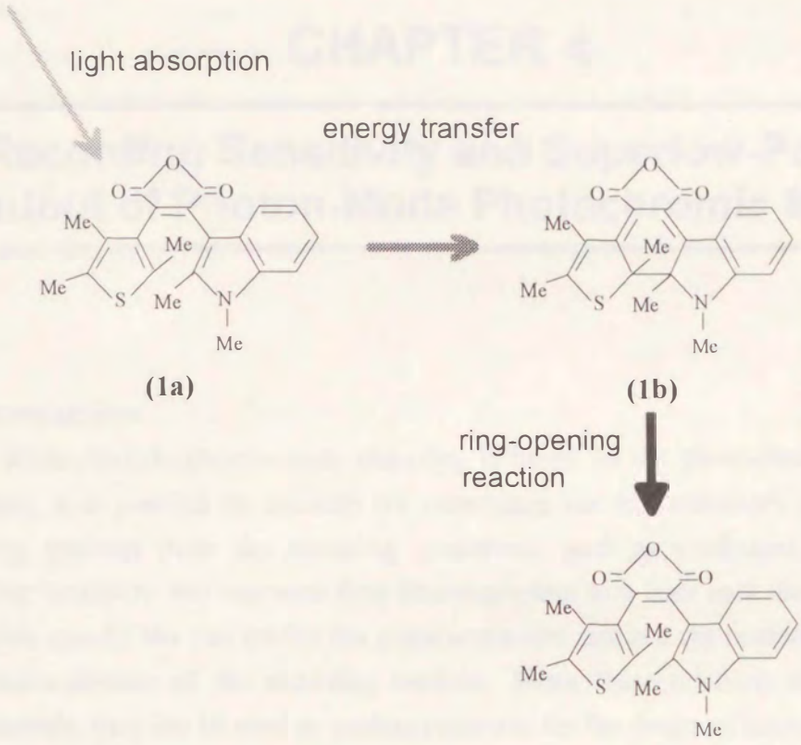

Figure 3-5. Model for increasing ring-opening sensitivity with time.

CHAPTER 4

Recording Sensitivity and Superlow-Power Readout of Photon-Mode Photochromic Memory

4.1 Introduction

Photochromic photon-mode recording is based on the photochemical reaction. Therefore, it is possible to estimate the reflectance (or transmittance) change of the recording medium from the recording conditions, such as irradiation laser power, recording sensitivity and exposure time (corresponding to a laser spot diameter divided by relative speed). We can predict the possible transfer rate and the readout repeatability from characteristics of the recording medium. When these relations are formulated quantitatively, they can be used as guiding principles for the design of memory media and system application. Some theoretical treatments have been carried out by Tomlinson,[11][13] but the definite relations have not yet been established. The purpose of this chapter is to formulate the theory to obtain the quantitative relation between recording sensitivity and possible data transfer rate.

One of the disadvantages of photon-mode photochromic recording is that the recorded information is destroyed by repeated readout operations. To solve this problem, two readout methods have been proposed.

(1) Use of readout light which is not absorbed by the photochromic material. The recorded information written by optical property changes, such as refractive index, birefringence or optical rotatory power, can be read with light of wavelengths longer than the absorption band of the photochromic materials.[41][59][60]

(2) Use of photochromic materials with a gated photochemical reactivity. Gated reactivity is the property that irradiation with any wavelength causes no photoreaction, while the reaction occurs when another external stimulation, such as heat, electric field or chemicals, is present.[7][15][16][27][46][61]

However, these two methods have the following problems. The first method loses the multi-wavelength recording capability, because the readout light can not distinguish

the different photochromic dyes. For the second method, it is difficult to form such photochromic compounds.

We propose here a new readout method which uses a superlow-power laser. This method provides sufficient readout repeatability for practical use, and is free of the above-mentioned problems.

4.2 Theoretical Formulation

4.2.1 Model of Reflectance Change

The memory medium has the structure shown in Fig. 4-1. Figure 4-2 shows the absorption spectrum of the recording layer. An initial state 1 is shown by a solid line and recorded state 2 is shown by a broken line. Assuming that the molecule corresponding to state 1 only absorbs at wavelength λ, the reflectance R is expressed as

$$R = \exp(-2.303\varepsilon C 2L) \tag{4-1}$$

Here, we assume perfect reflectance of the reflective layer.

When we irradiate the medium with wringing light (power P, wavelength λ) for an infinitesimal time dt, the medium absorbs the following number of photons:

$$dn = \frac{P\lambda}{hc}(1 - R)dt . \tag{4-2}$$

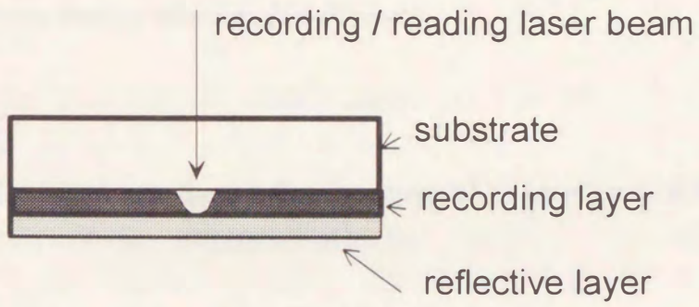

Figure 4-1. The structure of the photochromic memory medium. The recording layer contained photochromic molecules.

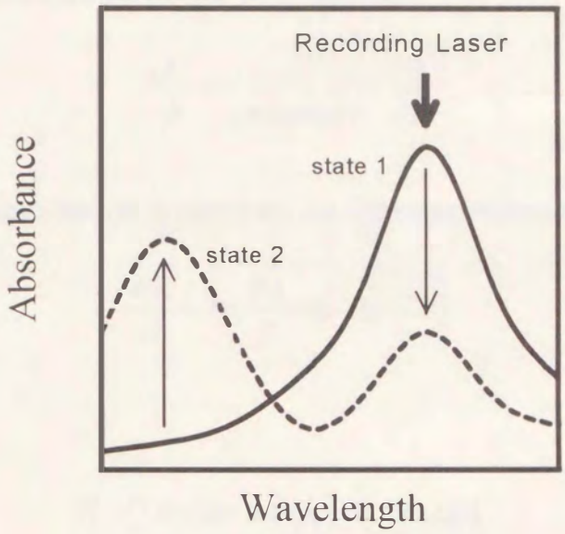

Figure 4-2. Absorption spectral change of a recording layer by irradiation with laser of wavelength λ. Solid line indicates initial state 1 and broken line indicates recorded state 2.

Then, the following number of molecules dN reacts:

$$dN = dn \cdot \phi . \tag{4-3}$$

The number of molecules in the irradiated volume LS is equal to $C \cdot LS \cdot N_a \cdot 10^{-3}$. The number of reaction molecules is therefore given by

$$dN = dC \cdot LSN_a \times 10^{-3} \tag{4-4}$$

Substituting eq. (4-2) as dn of eq. (4-3) and using eq. (4-4), we obtain the following equation.

$$\frac{\partial C}{\partial t} = \frac{-P\lambda}{hc} \cdot \frac{1}{LSN_a 10^{-3}} \cdot \phi (1 - R) . \tag{4-5}$$

On the other hand, the derivative of eq. (4-1) leads to

$$\frac{\partial C}{\partial t} = \frac{1}{-4.606\varepsilon LR} \cdot \frac{\partial R}{\partial t}. \tag{4-6}$$

From the above eqs. (4-5) and (4-6), the following differential equation with R is deduced:

$$\frac{\partial R}{\partial t} = 2\alpha \frac{P\lambda}{S} \cdot \varepsilon\phi \cdot R(1-R). \tag{4-7}$$

Then,

$$R = [1 + const. \times \exp(-2\alpha F\lambda \cdot \varepsilon\phi)]^{-1}. \tag{4-8}$$

The integral constant is determined by the initial reflectance R_{ini}

$$R_{ini} = [1 + const.]^{-1}, \tag{4-9}$$

and the total irradiation flux F is defined by

$$F \equiv P \cdot t / S. \tag{4-10}$$

Equation (4-8) expresses the irradiation (F) dependence of the reflectances. In the writing process, a pulsed laser (pulse width t_W) converts the initial reflectance R_{ini} to R_{mark}. The difference in the reflectance, R_{ini} and R_{mark}, is monitored in the readout process, and the inverse of the pulse width is the data transfer rate. The pulse width t_W corresponds to (laser spot diameter)/(relative speed). In the readout operation, the medium is continuously irradiated with a reading laser. The laser flux quantity is determined by the readout laser power, the diameter of the laser spot and the relative speed. During the reading process, the reflectance changes according to eqs. (4-8), (4-9) and (4-10). It is possible to derive the relationships among the writing laser power, the relative speed, the recording sensitivity and the data transfer rate. The relationships among the readout laser power, the readout cycles and the signal decline can also be calculated from the same equations.

4.2.2 Recording Sensitivity and Data Transfer Rate

Figure 4-3 shows the reflectance R and the differential $\partial R / \partial F$ as a function of the light flux F when $\varepsilon\phi$ =1000 $M^{-1}cm^{-1}$ and λ=633 nm. As can be seen from the figure, the most effective recording process, in which a maximum reflectance change is induced by a minimum light flux, is attained when R is around 0.5. The figure also shows that infinite light flux is required to bleach perfectly the recorded mark and that low R_{ini} of the land area requires large recording flux. Therefore such a mark and land are not suitable for effective writing.

Maximum data transfer rate $\mathbf{R_b}$ bps is derived as follows. In the recording process P is replaced with recording laser power P_{rec}. The data transfer rate $\mathbf{R_b}$ is expressed by the inverse time t_W^{-1} from eqs. (4-8), (4-9) and (4-10).

$$\mathrm{R_b} = 2\alpha \frac{P_{rec}}{S} \lambda\varepsilon\phi \cdot \ln\left(\frac{(1-R_{ini})R_{mark}}{(1-R_{mark})R_{ini}}\right)^{-1} \tag{4-11}$$

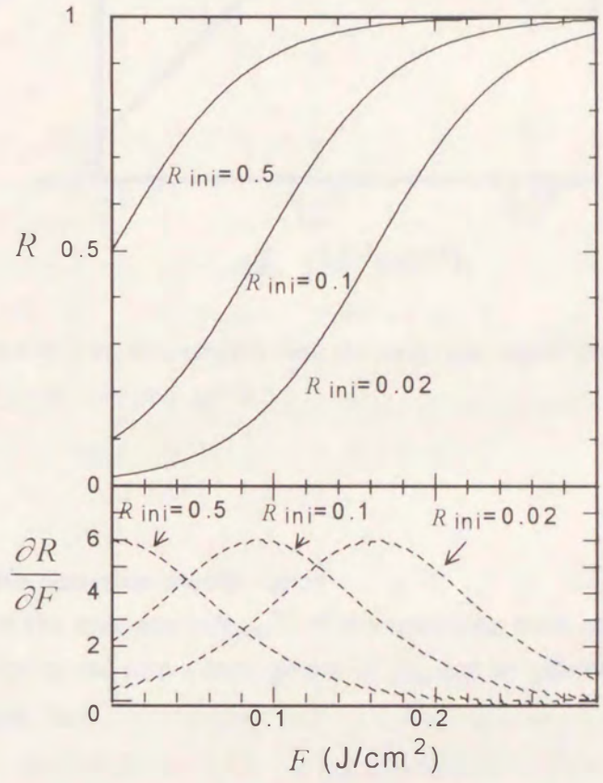

Figure 4-3. The reflectance R calculated by eqs. (4-7) and (4-8) under the conditions of λ=633 nm and $\varepsilon\phi$=1000 $M^{-1}cm^{-1}$.

Supposing that the reflectance change ($\Delta R \equiv R_{mark} - R_{ini}$) is 0.3, the highest recording efficiency is achieved by the reflectance R_{ini}=0.35 and R_{mark}=0.65 owing to large $\partial R / \partial F$, as shown in Fig. 4-3. Under the conditions of P_{rec}=10 mW, λ=633 nm, numerical aperture of objective lens NA=0.5 and laser spot area $S = \pi(\lambda / 2NA)^2$, we obtain the relationship between the material sensitivity $\varepsilon\phi$ and the transfer rate $\mathbf{R_b}$ shown in Fig. 4-4. For a typical value of $\varepsilon\phi$=1000 $M^{-1}cm^{-1}$, $\mathbf{R_b}$ is more than 10 Mbps.

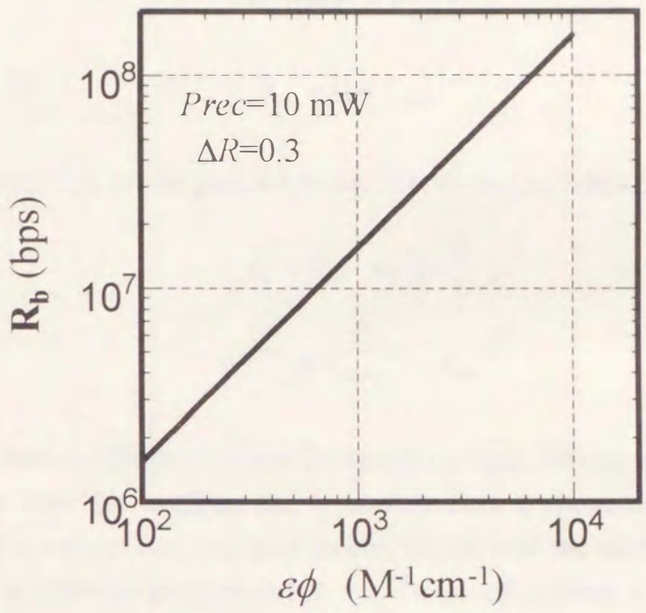

Figure 4-4. The data transfer rate $\mathbf{R_b}$ under the typical conditions λ=633 nm, P_{rec}=10 mW and ΔR=0.3.

4.2.3 Readout with Superlow-Power Laser

Changes of the reflectance $R_{mark}^{(m)}$ of the recording mark and $R_{ini}^{(m)}$ of the land after m readout operations with a laser power of P_{rep} can be calculated using eq. (4-8). The signal decreases as

$$R_{mark}^{(m)} = \left[1 + \Gamma_{mark} \cdot \exp(-2\alpha \frac{P_{rep} t_W}{S} m\lambda\varepsilon\phi)\right]^{-1}, \quad (4\text{-}12)$$

$$R_{ini}^{(m)} = \left[1 + \Gamma_{land} \cdot \exp(-2\alpha \frac{P_{rep} t_W}{S} m\lambda\varepsilon\phi)\right]^{-1}, \quad (4\text{-}13)$$

where the constants Γ_{mark} and Γ_{land} are defined by

$$R_{mark} \equiv (1 + \Gamma_{mark})^{-1} \quad (4\text{-}14)$$

$$R_{ini} \equiv (1 + \Gamma_{land})^{-1} \quad (4\text{-}15)$$

The signal current I_S from the photo-detector after m readout operations is

$$I_S = P_{rep} \cdot \gamma\eta \cdot \Delta R^{(m)} \quad (4\text{-}16)$$

$$\Delta R^{(m)} \equiv R_{mark}^{(m)} - R_{ini}^{(m)} \quad (4\text{-}17)$$

where γ is the pickup efficiency defined by the ratio of light arriving at the photodiode and light reflected from the medium, and η is photoelectric conversion efficiency of the photodiode. If we adopt very low laser power, we can read the memory many times; the readout cycle is inversely proportional to P_{rep}. However, in practice the lowest value of P_{rep} is determined by the signal to noise ratio. As mentioned above, the signal level is obtained from P_{rep} and $\Delta R^{(m)}$, but noise has various origins. Here we consider three principal noise sources: media noise which is caused by roughness of the recording layer surface; thermal noise which is caused by thermal disturbance of the electrons in photocurrent; and shot noise which is caused by quantum fluctuation of photons detected by photodiode. [62]-[65]

Figure 4-5 shows the dependence of the signal and the noise electric power on P_{rep}. The signal current I_S is proportional to P_{rep} and the signal power *Signal* decreases by 20 dB/decade. Medium noise current I_{nm} is also proportional to P_{rep} and the medium noise power N_m decreases similarly to *Signal*.[62] Therefore the signal-to-noise ratio *SNR* is constant when the readout laser power P_{rep} is greater than about the order of 1 μW. The medium noise power is generally much higher than thermal noise power N_t and shot noise power N_s. When the readout laser power decreases below about the order of 1 μW, *SNR*

is severely restricted by thermal noise for the first time. However this restriction is not fatal in principle. We are able to overcome this thermal noise limit by using a photodetection method which has a photocurrent self-amplificational function, for example, by using an avalanche photodiode or a coherent (heterodyne/homodyne) detection method.[63]-[65]

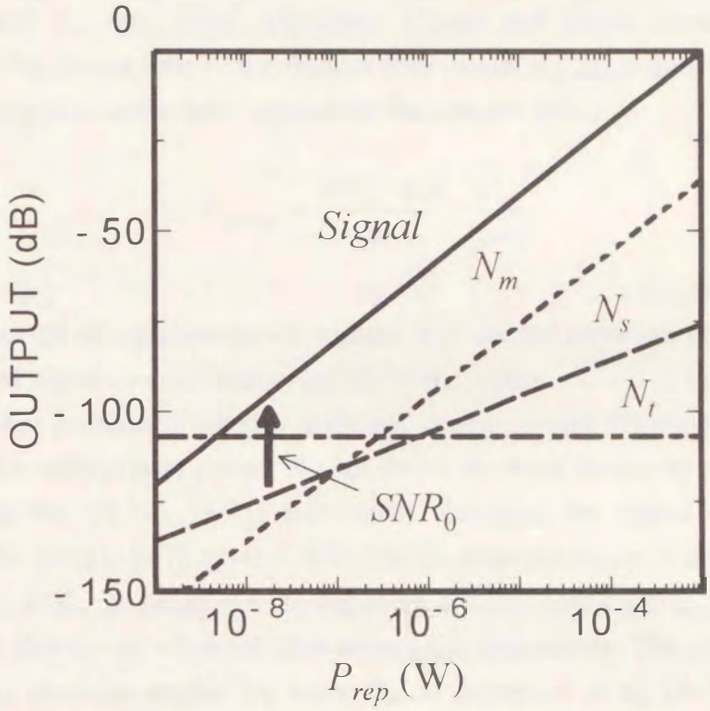

Figure 4-5. The laser power dependence of the signal and noise intensities. *Signal*, N_m, N_s and N_t are signal output level, the medium noise level, the shot noise level and the thermal noise level, respectively. SNR_0 indicates signal-to noise ratio required for the system.

Next, below 10^{-7} (W), *SNR* is restricted by shot noise N_s. The shot noise current I_{ns} is given as

$$I_{ns} = \sqrt{2eB \cdot \eta\gamma \cdot P_{rep} \cdot R_{ave}} \tag{4-18}$$

where B is bandwidth of the system and $R_{ave} = (R_{mark} + R_{im})/2$ is the average reflectance of the mark and land portion on the medium. The ratio $(I_s/I_{ns})^2$ obtained from eqs. (4-16)

and (4-18) gives the shot-noise-limited signal-to-noise (power) ratio SNR_{ns}, and eq. (4-19) is derived:

$$P_{rep} = \frac{SNR_{ns} \cdot 2eB}{\eta\gamma} \cdot \frac{R_{ave}}{(\Delta R)^2} \tag{4-19}$$

where ΔR and R_{ave} are initial reflectance change and initial average reflectance, respectively. The lowest limit of the readout laser power $P_{rep(\min)}$ is given by substituting SNR_{ns} as the signal-to-noise ratio required for the system (SNR_0).

$$P_{rep(\min)} = \frac{SNR_0 \cdot 2eB}{\eta\gamma} \cdot \frac{R_{ave}}{(\Delta R)^2} \tag{4-20}$$

The major concept of superlow-power readout is to use the minimum laser power while maintaining the signal-to-noise ratio required for the system.

Our next problem is whether sufficient readout cycles for practical use can be obtained by the readout laser power. We can derive the signal decline by super low power readout using eqs. (4-12), (4-13) and (4-20). Adopting the typical values ΔR=0.3, SNR_0=400 (26 dB),[66][67] η =0.4 A/W (for Si photodiode), γ =0.8 and B=5 MHz corresponding to $\mathbf{R_b}$=10 Mbps, the readout repeatability is calculated as shown in Fig. 4-6. The figure also shows the initial reflectance (R_{ini}) dependence. The minimum readout power $P_{rep(\min)}$ becomes smaller for lower R_{ini} as expressed in eq. (4-20). (R_{ave}=R_{ini} + ΔR/2) As can be seen from the figure, it is effective to reduce R_{ini} for increasing number of readouts. If we define the readout repeatable cycles as that when the signal level is decreased by 3 dB, more than 10^5 readout operations can be achieved for R_{ini}=0.6.

However it increases to about 10^6 cycles upon lowering R_{ini} (increasing optical density of recording layer). Furthermore, in the case that the optical density is very high, the signal does not show a monotonous decrease but a temporally increase at high readout cycles. This phenomenon occurs because eq. (4-7) is nonlinear and $R_{mark}^{(m)}$ increases faster than $R_{ini}^{(m)}$.

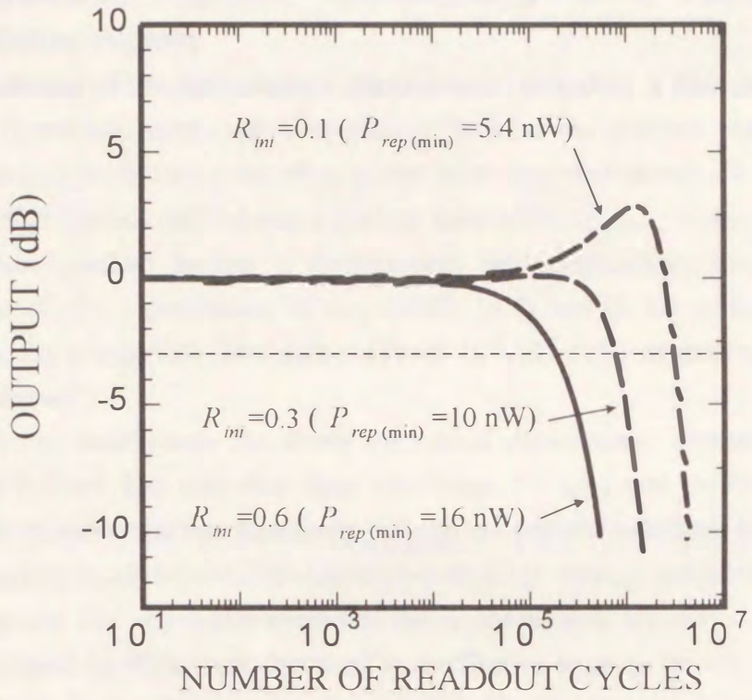

Figure 4-6. Readout cycle dependence of signal levels. The signal output depends on the initial reflection R_{ini} and minimum readout laser power $P_{rep(min)}$.

4.3 Superlow-Power Readout Characteristics of a Photochromic Diarylethene Medium

One of the problems of the photochromic photon-mode recording is that the recorded information is destroyed during readout operations. To solve this problem, we previously proposed a method which uses a superlow-power laser (superlow-power (SLP) readout method). The SLP readout method uses a readout laser power ($P_{rep(\min)}$ in eq. (4-20)) and a photodetection method having a photocurrent self-amplification function (e.g., avalanche photodiode). Combination of eqs. (4-20), (4-8) and (4-10) predicts 10^5-10^6 readout cycles for a superlow laser power (about 10^{-9}-10^{-7} (W)) depending upon the initial optical density.

In order to demonstrate the above theoretical expectations, experiments were carried out as follows. The recording layer (thickness: 0.5 μm) was prepared by spin coating a cyclohexanone solution containing polystyrene and photochromic diarylethene, 2-(1-octyl-2-methyl-3-indolyl)-3-(2,3,5-trimethyl-3-thyenyl) maleic anhydride, onto a glass disc substrate. The absorption spectra of the recording layer are shown in Fig. 4-7. Vacuum evaporated Ag films were deposited as a reflective layer on the recording layer to obtain the media having the structure shown in Fig. 4-1. The compound converts from the open to the closed ring form (from an uncolored state (solid line) to a colored state (broken line) in Fig. 4-7) upon irradiation with 450-500 nm light. The photogenerated colored form converts to the open ring form upon irradiation with 550-700 nm light. We therefore carried out recording by photobleaching of the precolored state and reading by detecting the reflectance changes with a 633 nm HeNe laser. In order to investigate the optical density (*OD*) dependence, we prepared two samples: by changing the concentration of the photochromic compound, one had an *OD* of 0.5 and the other had an *OD* of 0.15 at 633 nm in the colored state.

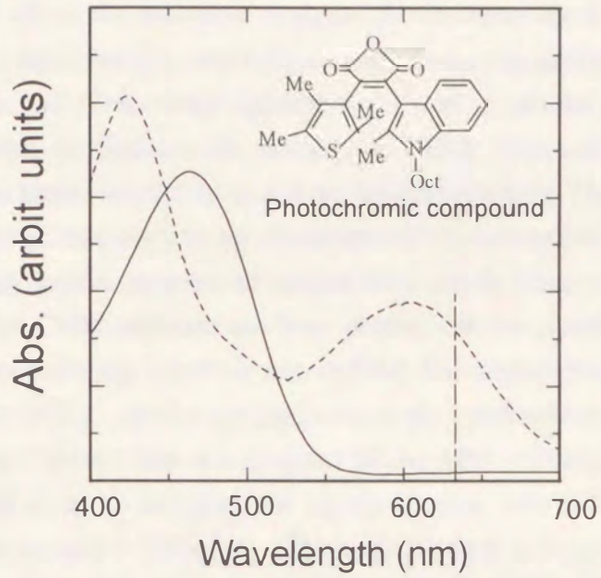

Figure 4-7. Absorption spectra of 2-(1-octyl-2-methyl-3-indolyl)-3-(2,3,5-trimethyl-3-thyenyl)maleic anhydride dispersed in polystyrene films. The solid line and the broken line indicate the open-ring and closed-ring forms, respectively.

Table 4-I. Write/read conditions.

Laser wavelength (nm)	633
Writing power (mW)	2.0
Reading power (mW)	10^{-5}-10^{-2}
Recording signal frequency (kHz)	300
Relative speed (m/s)	1.4

Figure 4-8 shows the apparatus employed for the experiment. It should be noted that a focal servo system using a near-infrared laser diode was adopted in this apparatus to avoid the destruction of recording signals during focusing, and the signal detection was carried out by using an Si-avalanche photodiode (APD; Hamamatsu Photonics K.K. S5343), which has higher sensitivity at a short light wavelength. The 633 nm laser was modulated to a certain frequency by an acoustooptical modulator (AOM) and introduced to a pickup optical system through an optical fiber which conserves polarization. A neutral density filter (ND) regulated the laser power. In the pickup system, two laser beams were superposed using a dichroic mirror (DM) and focused into the same spot by a single objective lens (OL). In the reading process, the beam reflected from the medium passed through the objective lens was detected by the APD. The gain of the APD was controlled properly so as to maximize the carrier-to-noise ratio (CNR). The write/read conditions are summarized in Table 4-I. The readout power in the range of 10 μW to 10 nW was used to examine the readout laser power dependence of the CNR.

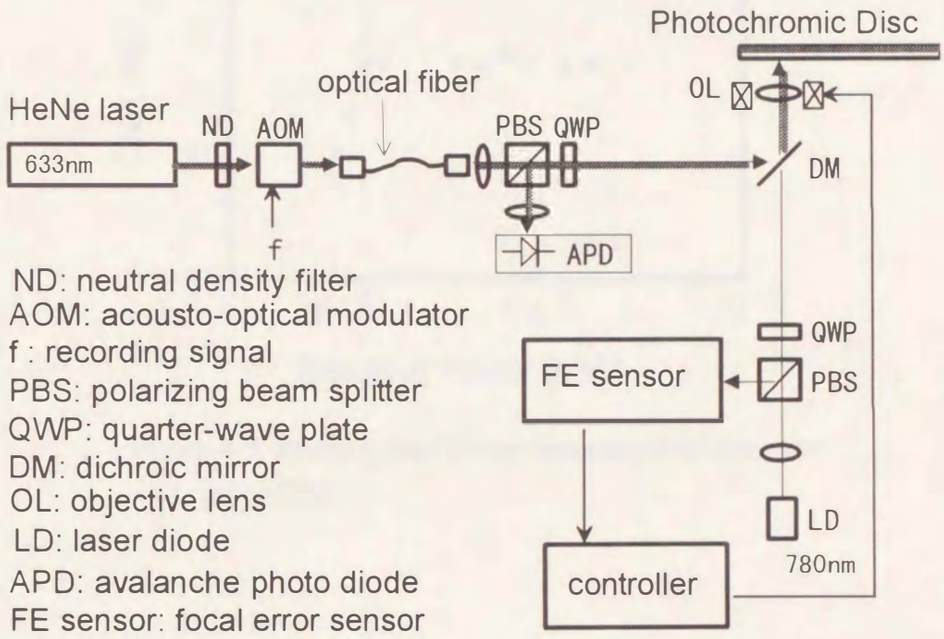

Figure 4-8. The apparatus for SLP readout.

Figure 4-9 shows the readout laser power dependence for the *OD*=0.5 sample. The CNR is constant when the readout laser power is greater than 20 nW, and it is restricted by the media noise. On the other hand, the CNR decreases rapidly when the power is less than 20 nW, and it is restricted by the shot noise. Therefore, to obtain CNR of 45 dB in the system, a superlow minimum laser power of around 20 nW is required. Figure 4-10 shows the readout cycle dependence of carrier levels by the SLP readout method. In this measurement the write/read conditions were set to the values shown in Table 4-I except for a fixed readout power of 20 nW. On condition of keeping the carrier level decrease less than 3 dB, the 10^5 cycle readout operation for the *OD*=0.15 sample and 10^6 cycles for the *OD*=0.5 sample are possible by the SLP readout method.

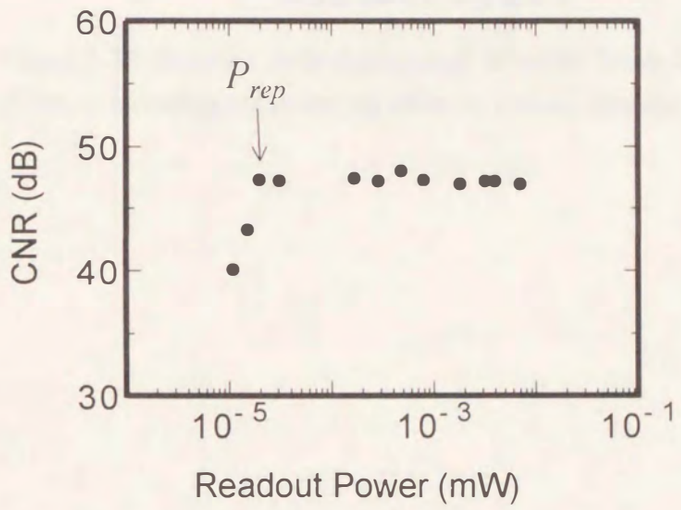

Figure 4-9. Readout laser power dependence of carrier to noise ratio (CNR).

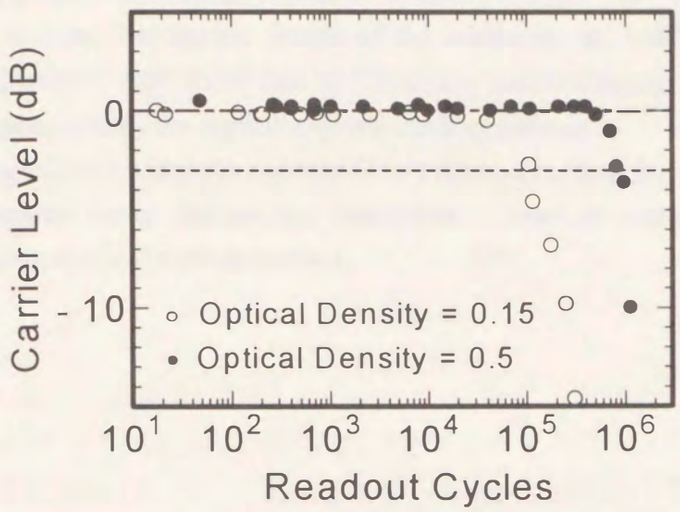

Figure 4-10. Readout cycle dependence of carrier levels for two different recording media having different optical densities

4.4 Conclusion

We proposed the superlow-power readout method for a photon-mode photochromic medium. For typical values of the sensitivity $\varepsilon\phi$ =1000 $M^{-1}cm^{-1}$ and recording laser power 10 mW, more than 10 Mbps data transfer rate and 10^5-10^6 readout operations was predicted by the superlow-power readout method.

We demonstrated a superlow-power (SLP) readout method for a photochromic diarylethene medium using diarylethene derivatives. Readout cycles of 10^6 were performed by using the SLP readout method.

CHAPTER 5

Multi-Wavelength Recording and a New Method of Crosstalk Reduction

5.1 Introduction

Photon-mode recording, which uses photoreactions of molecules in the memory media, have a potential to make use of specific characteristics of light, such as wavelength, polarization and phase, for multiplex recording. One of the candidates for erasable photon-mode optical recording is photochromic materials.[14][18] An approach to increase the memory density is multi-wavelength recording (or multi-frequency recording). A medium consisting of multilayer (or a layer) which contain photochromic materials with different absorption bands has been used for the multi-wavelength recording.[16][20] Each layer is irradiated independently by the corresponding wavelength laser for recording, and the memory is read by a laser beam of the same wavelength.

For multi-wavelength recording, it was believed that each layer containing photochromic material should have a narrow absorption band to avoid crosstalk. This is the reason why J-aggregate of spiropyrans was examined as a candidate of multiplex memory materials. The spiropyrans, however, have poor durability.[17] For practical application, the photochromic materials should remain stable even after many write/erase operations. Photochromic materials with sufficient durability are diarylethene derivatives with heterocyclic rings.[26] These compounds, however, have broad absorption bands which make it difficult to use them for multi-wavelength recording media.

The purpose of this chapter is to reveal the mechanism of crosstalk between multiple channels, and to propose a new crosstalk reduction method which can be applicable to photochromic materials with broad bands such as diarylethene derivatives.

5.2 Theoretical Analysis of the Crosstalk

We consider, for simplicity, two-wavelength recording using two photochromic materials, A and B, with different absorption maxima at λ_1 and λ_2, as shown in Fig. 5-1. At λ_1 both compounds A and B have absorption bands, the absorption intensity of compound B being weaker than that of compound A. At λ_2 compound B has stronger absorption than compound A. Coexistence of the two absorption bands at the writing/reading wavelength causes crosstalk. The signal written by a λ_1 laser is mixed with the signal written by a λ_2 laser, and the reflectance varies into four levels, not two levels.

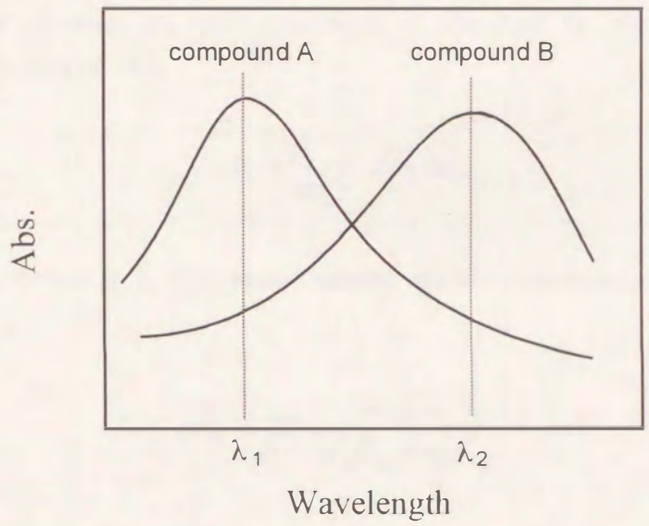

Figure 5-1. A schematic illustration of the spectra of two photochromic compounds with different absorption bands.

The readout signal by the λ_1 laser includes the following two origins of crosstalk.

1. ***Crosstalk in the writing process***
   Not only the λ_1 laser but also the λ_2 laser can induce the photochromic reaction of molecule A. Therefore, the decrease of absorbance at λ_1 includes the effect of the writing process by the λ_2 laser.
2. ***Crosstalk in the reading process***

The absorbance change at λ_1 includes the effect due to the photoreaction of compound **B**, because compound **B** has an absorption band at λ_1.

The crosstalk originates from *1* and *2*. Now, we consider that two laser beams, λ_1 and λ_2, irradiate the recording layer containing materials **A** and **B**. We assume that the absorbance of the recording layer is lower than 0.2. (That is, we adopt thin *OD* approximation.) By using the Lambert-Beer law, the absorption Apt_i at λ_i is expressed by

$$Apt_i \approx 2.303 \cdot L\left(\varepsilon_{Ai} C_A + \varepsilon_{Bi} C_B\right). \tag{5-1}$$

The number of photons dn_i with wavelngth λ_i absorbed by the layer during an infinitesimal time interval dt is

$$dn_i = \frac{\lambda_i}{hc} \cdot P_i \, Apt_i \, dt, \tag{5-2}$$

where P_i is laser power at λ_i. The photon number absorbed by molecule X in the layer is expressed as

$$dn_{Xi} = dn_i \cdot \frac{\varepsilon_{Xi} C_X}{\varepsilon_{Ai} C_A + \varepsilon_{Bi} C_B}. \tag{5-3}$$

According to the Stark-Einstein law, the total number dN_X of reacting molecules X is

$$dN_{iX} = \sum_{i=1,2} dn_i \, \phi_{Xi}. \tag{5-4}$$

The relationship between molarity and molecular number is

$$N_X = C_X S L N_a 10^{-3}, \tag{5-5}$$

where S is the area of the irradiating laser spot. Combining eqs.(5-1) (5-2) (5-3) and (5-4), and transforming the variable to C_X from N_X by eq. (5-5), we obtain the following differential equation (5-6):

$$\frac{\partial C_X}{\partial t} = -\alpha \frac{1}{S} \sum_{i=1,2} P_i \lambda_i \varepsilon_{Xi} \phi_{Xi} \cdot C_X. \tag{5-6}$$

By integrating from t=0 to t=t_W, the solution is

$$C_X(t_W) = C_X(0)\exp\left(-(\beta_{X1}P_1 + \beta_{X2}P_2)\right), \tag{5-7}$$

where

$$\beta_{Xi} \equiv \frac{\alpha}{S}\cdot\varepsilon_{Xi}\,\phi_{Xi}\,\lambda_i\,t_W, \tag{5-8}$$

β_{Xi} corresponds the recording efficiency and t_W expresses writing pulse width.

Figure 5-2 shows the construction of the memory medium. The recording layer of thickness L is a mixture of two photochromic compounds A and B with different absorption bands, and reflectance of the reflecting layer is assumed to be perfect. The writing laser is on-off modulated by frequency ω_1 at λ_1 and by frequency ω_2 at λ_2. As a result, time-dependent total reflectance R_i at the wavelength λ_i is expressed as

$$R_i = 1 - 2.303\cdot 2L\sum_{X=A,B}\varepsilon_{Xi}C_X(0)\exp\left(-\sum_{j=1,2}\beta_{Xj}P_j\theta(\cos\omega_j t)\right) \tag{5-9}$$

where θ represents the step function.

When the reflectance is read by the λ_1 laser, the $\beta_{A2}P_2\theta$ (cos $\omega_2 t$) term in the exponent corresponds to the crosstalk of the writing process, and the term $\varepsilon_{Bi}C_B(0)\exp(-\beta_{B1}P_1\theta(\cos\omega_1 t)-\beta_{B2}P_2\theta(\cos\omega_2 t))$ corresponds to the crosstalk of the reading process. The reflectance R_i takes four values $R_i^{(\mu)}$ (μ=0,1,2,3) depending on the power modulation of the writing laser $P_j\theta$ (cos$\omega_j t$) (j=1,2). For example, $R_i^{(0)}$, $R_i^{(1)}$, $R_i^{(2)}$ and $R_i^{(3)}$ indicate the reflectances of the unirradiated portion, the portion irradiated by only λ_1 wavelength light, by only λ_2 wavelength light and by both λ_1 and λ_2 wavelength light, respectively. The readout signal is proportional to the reflectance R_i in the long-mark approximation (the recording mark length is larger than the laser spot diameter). For simplicity, we ignore this proportional coefficient. CH1 output read by irradiating the wavelength λ_1 laser is proportional to the reflectance at λ_1. This signal (O_{1OUT}) contains the following four kind of components: DC (O_{1DC}), frequency ω_1 (O_{1S}), frequency ω_2 (O_{1LC}) and frequency $\omega_1 \pm \omega_2$ (O_{1NC}).

$$O_{1OUT} = O_{1DC} + O_{1S}\cos\omega_1 t + O_{1LC}\cos\omega_2 t + O_{1NC}\cos\omega_1 t\cdot\cos\omega_2 t. \tag{5-10}$$

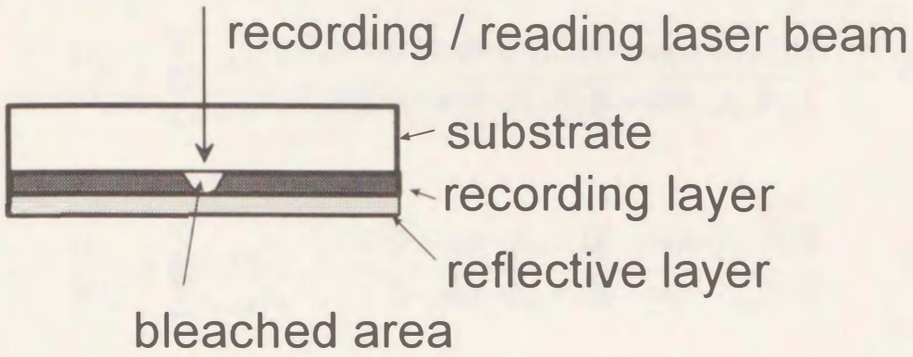

Figure 5-2. Construction of a photochromic medium for multi-wavelength recording. The recording layer consists of a mixture of two kinds of photochromic compounds. Reflective layer is vacuum-deposited Ag film.

The third and fourth components are due to linear and nonlinear crosstalk. CH2 output using wavelength λ_2 laser has a similar form.

These components can be expressed by reflectance $R_i^{(\mu)}$ as

$$O_{iDC} = \frac{1}{4}\left(R_i^{(0)} + R_i^{(1)} + R_i^{(2)} + R_i^{(3)}\right), \tag{5-11}$$

$$O_{iS} = \frac{1}{4}\left(R_i^{(0)} + R_i^{(1)} - R_i^{(2)} - R_i^{(3)}\right), \tag{5-12}$$

$$O_{iLC} = \frac{1}{4}\left(R_i^{(0)} - R_i^{(1)} + R_i^{(2)} - R_i^{(3)}\right), \tag{5-13}$$

$$O_{iNC} = \frac{1}{4}\left(R_i^{(0)} - R_i^{(1)} - R_i^{(2)} + R_i^{(3)}\right), \tag{5-14}$$

where $R_i^{(0)} > R_i^{(1)} > R_i^{(2)} > R_i^{(3)}$.

In general, the crosstalk is expressed as a ratio to the main signal. By introducing eq. (5-9) into $R_i^{(\mu)}$, we obtain the crosstalk intensity for CH1 as follows.

Linear:

$$\frac{O_{1LC}}{O_{1S}} = \frac{\sum_{X=A,B} \varepsilon_{X1} C_X(0) \cdot \left(1+\exp(-\beta_{X1}P_1)\right)\left(1-\exp(-\beta_{X2}P_2)\right)}{\sum_{X=A,B} \varepsilon_{X1} C_X(0) \cdot \left(1-\exp(-\beta_{X1}P_1)\right)\left(1+\exp(-\beta_{X2}P_2)\right)}, \tag{5-15}$$

Nonlinear:

$$\frac{O_{1NC}}{2O_{1S}} = \frac{\sum_{X=A,B} \varepsilon_{X1} C_X(0) \cdot \left(1-\exp(-\beta_{X1}P_1)\right)\left(1-\exp(-\beta_{X2}P_2)\right)}{\sum_{X=A,B} \varepsilon_{X1} C_X(0) \cdot \left(1-\exp(-\beta_{X1}P_1)\right)\left(1+\exp(-\beta_{X2}P_2)\right)}. \tag{5-16}$$

The expressions for CH2 have similar forms.

Linear:

$$\frac{O_{2LC}}{O_{2S}} = \frac{\sum_{X=A,B} \varepsilon_{X2} C_X(0) \cdot \left(1+\exp(-\beta_{X2}P_2)\right)\left(1-\exp(-\beta_{X1}P_1)\right)}{\sum_{X=A,B} \varepsilon_{X2} C_X(0) \cdot \left(1-\exp(-\beta_{X2}P_2)\right)\left(1+\exp(-\beta_{X1}P_1)\right)}, \tag{5-17}$$

Nonlinear:

$$\frac{O_{2NC}}{2O_{2S}} = \frac{\sum_{X=A,B} \varepsilon_{X2} C_X(0) \cdot \left(1-\exp(-\beta_{X2}P_2)\right)\left(1-\exp(-\beta_{X1}P_1)\right)}{\sum_{X=A,B} \varepsilon_{X2} C_X(0) \cdot \left(1-\exp(-\beta_{X2}P_2)\right)\left(1+\exp(-\beta_{X1}P_1)\right)}. \tag{5-18}$$

We consider the case in which the crosstalk in the reading process is neglected, in order to compare the theoretical expression with the experimental one using two diarylethenes with different absorption maxima. In this case, eqs. (5-17) and (5-18) for CH2 are simplified as follows.

Linear:

$$\frac{O_{2LC}}{O_{2S}} = \frac{\left(1+\exp(-\beta_{B2}P_2)\right)\left(1-\exp(-\beta_{B1}P_1)\right)}{\left(1-\exp(-\beta_{B2}P_2)\right)\left(1+\exp(-\beta_{B1}P_1)\right)}. \tag{5-19}$$

Nonlinear:

$$\frac{O_{2NC}}{2O_{2S}} = \frac{\left(1-\exp(-\beta_{B1}P_1)\right)}{2\left(1+\exp(-\beta_{B1}P_1)\right)}. \tag{5-20}$$

The main signal component in CH2 output is as follows.

Main signal:

$$O_{2S} \propto \varepsilon_{2B} C_B(0) L \left(1-\exp(-\beta_{B2}P_2)\right)\left(1+\exp(-\beta_{B1}P_1)\right) \tag{5-21}$$

Now we obtain the relationships between recording parameter $\beta_{B2}P_2$ and each component, as shown in Fig. 5-3. Under a condition of $\beta_{B2}P_2$=1.2, which is about 3 dB below the saturation level of the main signal, we can estimate that the linear component of the crosstalk is about -2 dB and the nonlinear one is about -14 dB when $\beta_{B2}P_2 \sim 1$.

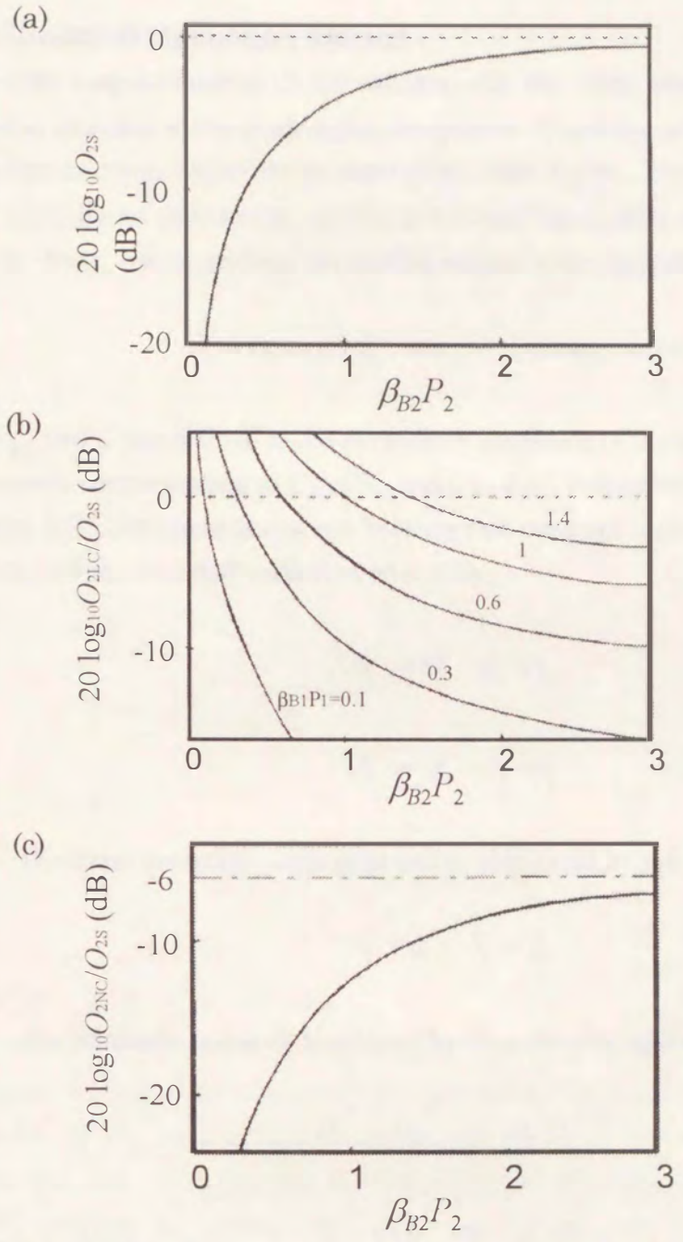

Figure 5-3. Relationships between the recording parameter $\beta_{B2}P_2$ and (a) the main signal component, (b) linear crosstalk component, and (c) nonlinear crosstalk component in CH2.

(a) Carrier level. We determined the typical recording conditions so that the carrier level was 3dB below the saturated value and $\beta_{B2}P_2$=1.2.

(b) The ratio of the linear crosstalk component to the main signal component was dependent on $\beta_{B1}P_1$ and $\beta_{B2}P_2$. Under the conditions of $\beta_{B2}P_2$=1.23 and $\beta_{B1}P_1$=1, the ratio was about -2 dB.

(c) The ratio of nonlinear to linear crosstalk components was dependent on $\beta_{B2}P_2$. This value was always smaller than -6 dB by the factor of 1/2. Under the condition of $\beta_{B2}P_2$=1.23 and $\beta_{B1}P_1$=1, this ratio was about -14 dB.

5.3 A Crosstalk Reduction Method

The output equation (5-10) indicates that the linear crosstalk component of one channel is included in the main signal component of another channel, and the nonlinear component is composed of the product of the main signals. These crosstalk components are reduced by an appropriate operation between the reading outputs of the multiplied channels. Now, we can express the reading output in the normalized form of

$$O_1 = \cos\omega_1 t + \xi_1 \cos\omega_2 t + \zeta_1 \cos\omega_1 t \cdot \cos\omega_2 t \,, \tag{5-22}$$

where ξ_1 and ζ_1 are defined as the normalized amplitude of linear and nonlinear crosstalk components corresponding to O_{1LC}/O_{1S} and O_{1NC}/O_{1S}, respectively. O_2 has a similar form. Here the DC component is ignored because that does not include any information. The following are the crosstalk reduction operations.

$$O_1' = O_1 - \delta_1 \cdot O_2, \tag{5-23}$$

$$O_2' = O_2 - \delta_2 \cdot O_1. \tag{5-24}$$

The linear crosstalk component can be eliminated by the choice of

$$\delta_1 = \xi_1, \quad \delta_2 = \xi_2. \tag{5-25}$$

The nonlinear crosstalk is reduced by the following operations.

$$O_1'' = O_1' - \sigma_1 \cdot O_1' O_2', \tag{5-26}$$

$$O_2'' = O_2' - \sigma_2 \cdot O_1' O_2'. \tag{5-27}$$

The nonlinear crosstalk component $\omega_1 + \omega_2$ can also be eliminated by the choice of σ_1 and σ_2, for example,

$$\sigma_1 = \frac{\zeta_1 - \xi_1\zeta_2}{\left(1 - \xi_1\xi_2\right)^2}, \quad \sigma_2 = \frac{\zeta_2 - \xi_2\zeta_1}{\left(1 - \xi_1\xi_2\right)^2}. \tag{5-28}$$

In this case, however, other components, such as $2\omega_1 + \omega_2$, $\omega_1 + 2\omega_2$, are newly

generated. Therefore, the parameters σ_1 and σ_2 should be optimized so that these newly generated components become as small as possible. The intensities of the components in CH1 output after operations (5-23), (5-24), (5-26) and (5-27) with the parameter choices (5-25) and (5-28) are expressed as follows.

ω_1 (main signal):

$$1-\xi_1\xi_2-\frac{(\zeta_1-\xi_1\zeta_2)^2}{2(1-\xi_1\xi_2)}, \tag{5-29}$$

ω_2 (linear):

$$\frac{(\zeta_1-\xi_1\zeta_2)(\zeta_2-\xi_2\zeta_1)}{2(1-\xi_1\xi_2)}, \tag{5-30}$$

$2\omega_1 \pm \omega_2$ (nonlinear):

$$\frac{(\zeta_1-\xi_1\zeta_2)(\zeta_2-\xi_2\zeta_1)}{4(1-\xi_1\xi_2)}, \tag{5-31}$$

$\omega_1 \pm 2\omega_2$ (nonlinear):

$$\frac{(\zeta_1-\xi_1\zeta_2)^2}{4(1-\xi_1\xi_2)}. \tag{5-32}$$

Other components (DC, $2\omega_1$, $2\omega_2$, $2\omega_1 \pm 2\omega_2$) are negligible because they are smaller than the above components. Because ξ_i and ζ_i are smaller than unity in general. ξ_i^2 and ζ_i^2 are much smaller than unity. Expressions (5-29)-(5-32) show that the crosstalk components are reduced to a considerable extent by these operations.

The crosstalk reduction method described above can be used for multi-wavelength recording even when the photochromic materials have broad absorption bands and poor wavelength selectivity. The method is also applicable to high-density multi-wavelength recording with the use of photochromic materials with narrower absorption bands.

5.4 Two-Wavelength Recording using Diarylethenes

In order to demonstrate the usefulness of the above crosstalk reduction method for multi-wavelength recording, the following experiments were carried out. Two kinds of diarylethenes, 2,3-bis(2-methylbenzo[b]thiophen-3-yl) maleic anhydride (compound A) and 2-(1,2-dimethyl-3-indolyl)-3-(2,3,5-trimethyl-3-thienyl) maleic anhydride (compound B), were dispersed in poly(vinyl butyral) (PVB) (15 wt.%) and used for the recording media. A Ag reflective layer was overcoated by vacuum evaporation.

The photochromic behavior of the compounds is shown in Fig. 5-4. Compound A converts from the open to the closed-ring form upon irradiation with 405 nm light. The photogenerated colored form converts to the open-ring form upon irradiation with light of wavelength longer than 500 nm. Bleaching of the longer-wavelength absorption can also be induced by irradiation with the 515 nm Ar ion laser. On the other hand, compound B converts from the open to closed-ring form upon irradiation with 490nm light, and the closed-ring form returns to the open-ring form upon irradiation with light longer than 550nm. Bleaching can also be induced with the 633nm He-Ne laser.

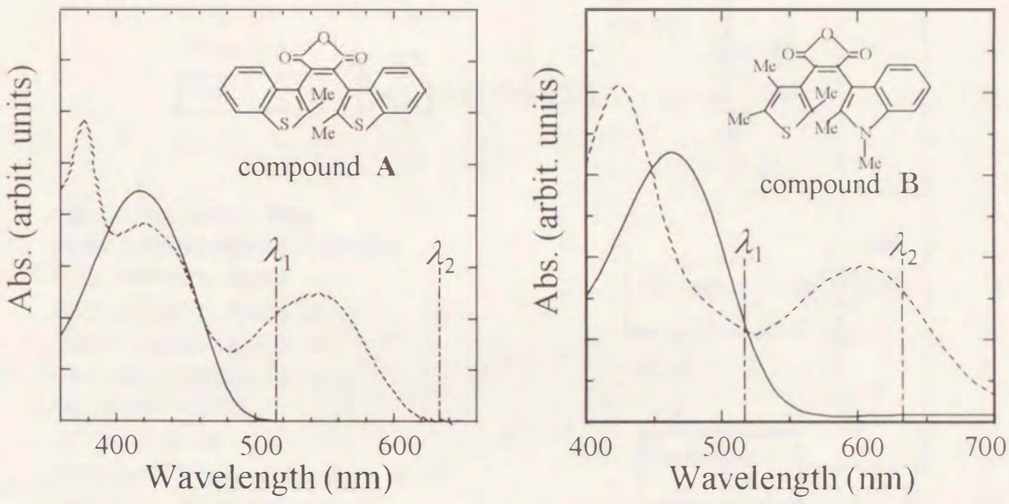

Figure 5-4. Absorption spectra of 2,3-bis(2-methylbenzo[b]thiophen-3-yl) maleic anhydride (compound A) and 2-(1,2-dimethyl-3-indolyl)-3-(2,3,5-trimethyl-3-thienyl) maleic anhydride (compound B) dispersed in poly(vinyl butyral) film.

Compound **A** has a very weak absorption at 633nm. This indicates that the crosstalk in the writing/reading process using 633nm light is negligible. At 515nm, on the

other hand, both compounds A and B show absorption. Table 5-I summarizes the writing sensitivities $\varepsilon_{Xi}\phi_{Xi}$ of compounds A and B dispersed in PVB. As can be seen from the table, the crosstalk induced in the writing process by 515nm light is as large as the main signal written by 633nm light.

Table 5-I. Recording sensitivities $\varepsilon_{Xi}\phi_{Xi}$ of compounds A and B dispersed in poly(vinyl butyral).

Compound	A		B	
Wavelength (nm)	515	633	515	633
$\varepsilon_{Xi}\phi_{Xi}$ ($M^{-1}cm^{-1}$)	1000	50	1300	1100

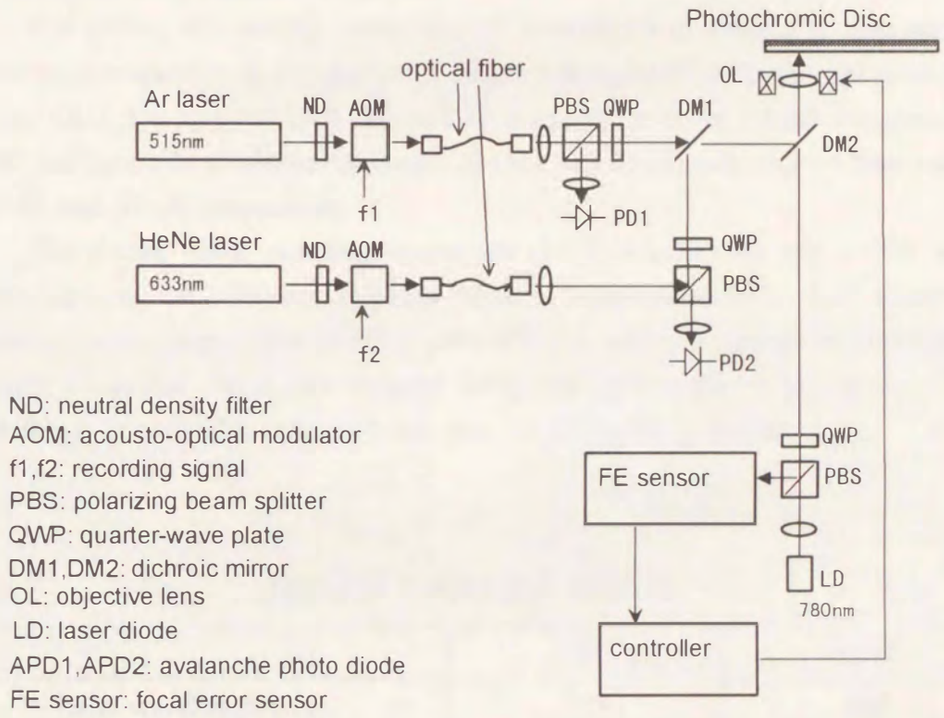

Figure 5-5. The apparatus for two-wavelength recording.

Figure 5-5 shows the apparatus for the multi-wavelength recording experiment. It is noted that a focal servo system using a near-infrared laser diode was adopted in this apparatus to avoid the destruction of signals during focusing. The 633nm and 515nm lasers were modulated to a certain frequency by acousto-optical modulators (AOM) and introduced to a pickup optical system through optical fibers which conserve polarization. In the pickup system, these three laser beams were superposed using two dichroic mirrors (DM1, DM2) and focused into the same spot by a single objective lens (OL). The diameter of this laser spot was about 2 μm. In the reading process, the beams reflected from the medium passed through the objective lens and were detected by PIN photodetectors (PD). The crosstalk reduction operation was carried out between these two PD outputs. The output signals before and after the crosstalk reduction operations were compared using a spectrum analyzer.

The writing and reading conditions are summarized in Table 5-II. The writing conditions correspond to $\beta_{B2}P_2=\beta_{B1}P_1=1.2$. Figure 5-6 shows the output power spectra of CH1 and CH2. The crosstalk (100 kHz) in CH1 is as small as about -24 dB. The crosstalk in CH2 has linear (80 kHz) and nonlinear (20 kHz, 180 kHz) components whose values are -2 dB and -14 dB, respectively.

The circuit which simulates operations (5-23),(5-24),(5-26) and (5-27) were constructed using the differential amplifier (National Semiconductor Co., Ltd.; LM6361) and analog circuit (Analog Devices Co., Ltd.; AD533). After the operations of crosstalk reduction using this circuit, we obtained the power spectra shown in Fig. 5-7. The crosstalk was considerably reduced to less than -25 dB by the operation.

Table 5-II. Write/read conditions

	CH1	CH2
Laser wavelength (nm)	515	633
Writing laser power (mW)	2.7	2.0
Reading laser power (mW)	0.1	0.1
Recording signal frequency (kHz)	80	100
Relative speed (m/s)	1.4	

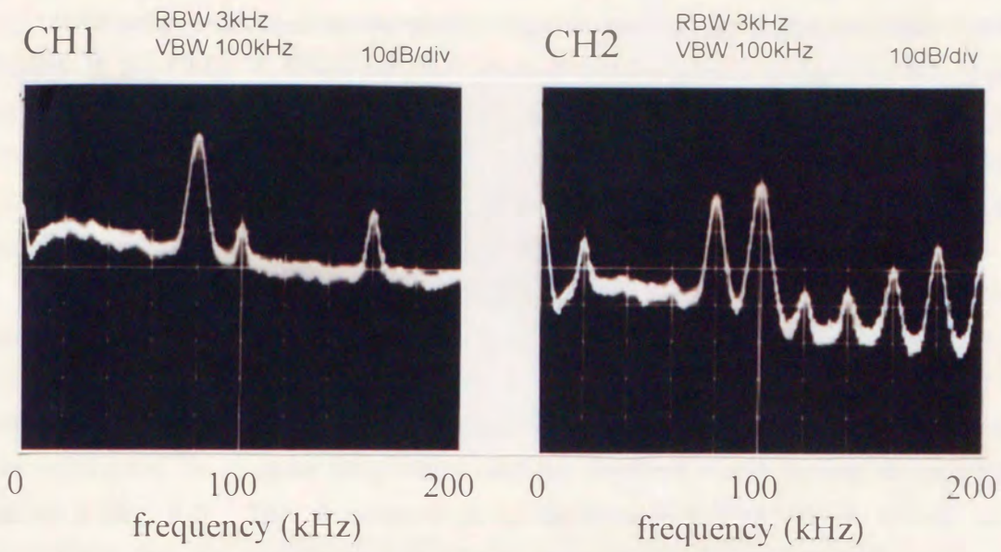

Figure 5-6. Output signal power spectra of CH1 and CH2 before crosstalk reduction operations.

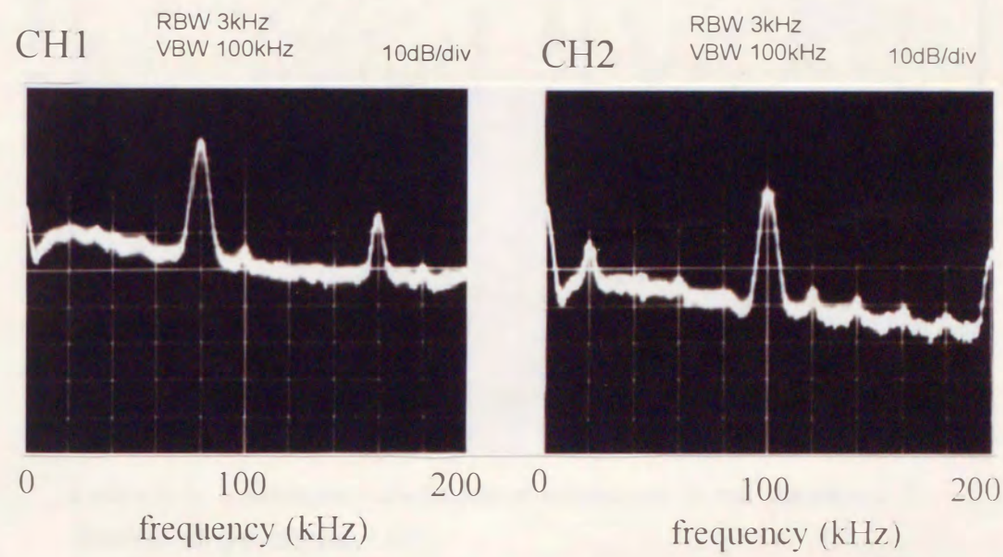

Figure 5-7. Output signal power spectra of CH1 and CH2 after crosstalk reduction operations.

5.5 Superlow-Power Readout of Multi-Wavelength Recording Medium

We proposed the superlow-power readout method for a photon-mode optical memory in the Chap. 4. Since the SLP readout method simply detects the absorption change of the medium at the readout laser wavelength, it can be applied easily to multi-wavelength recording. We have already analyzed the crosstalk in multi-wavelength recording and proposed a crosstalk reduction method. In this section we present the results obtained by applying the SLP readout method to two-wavelength recording.

Two kinds of diarylethenes, 2,3-bis(2-methylbenzo[b]thiophen-3-yl) maleic anhydride (compound A), and 2-(1-octyl-2-methyl-3-indolyl)-3-(2,3,5-trimethyl-3-thyenyl)maleic anhydride (compound B), as shown in Fig. 5-8, were dispersed in polystyrene and used for the recording layer (thickness: 0.7 μm). The Ag reflective layer was overcoated by vacuum evaporation and we obtained media having the structure shown in Fig. 5-1. The photoreactions of compounds A and B has already been illustrated in Sec. 5.4, and the write/read were carried out in the same manner.

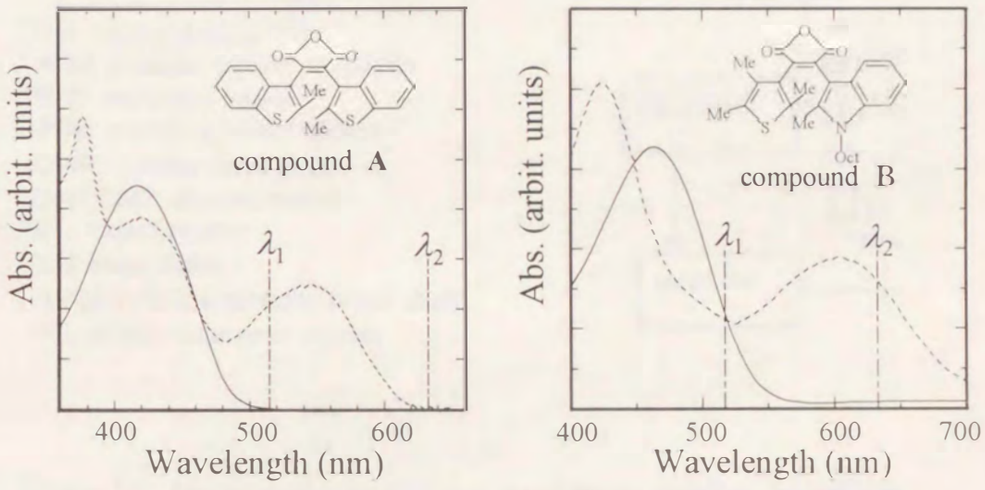

Figure 5-8. Absorption spectrums of compound A and compound B dispersed in polystyrene films

Figure 5-9 shows the apparatus employed for the SLP two-wavelength recording. Three lasers (515nm, 633nm and 780nm) were superposed using two dichroic mirrors (DMs) and focused into the same spot by a single objective lens (OL). In the reading process, the readout beams reflected from the medium were divided by the DMs and

detected by corresponding avalanche photodiodes (APDs). Crosstalk reduction operations were carried out between these two APD outputs. We compared the output signals before and after the crosstalk reduction operations, using a spectrum analyzer.

The write/read conditions are summarized in Table 5-III. In order to clarify the influence of multi-wavelength crosstalk, we recorded the different frequencies: 240 kHz in the Ar laser channel and 300 kHz in the HeNe laser channel. The readout laser powers were set at the superlow-power level.

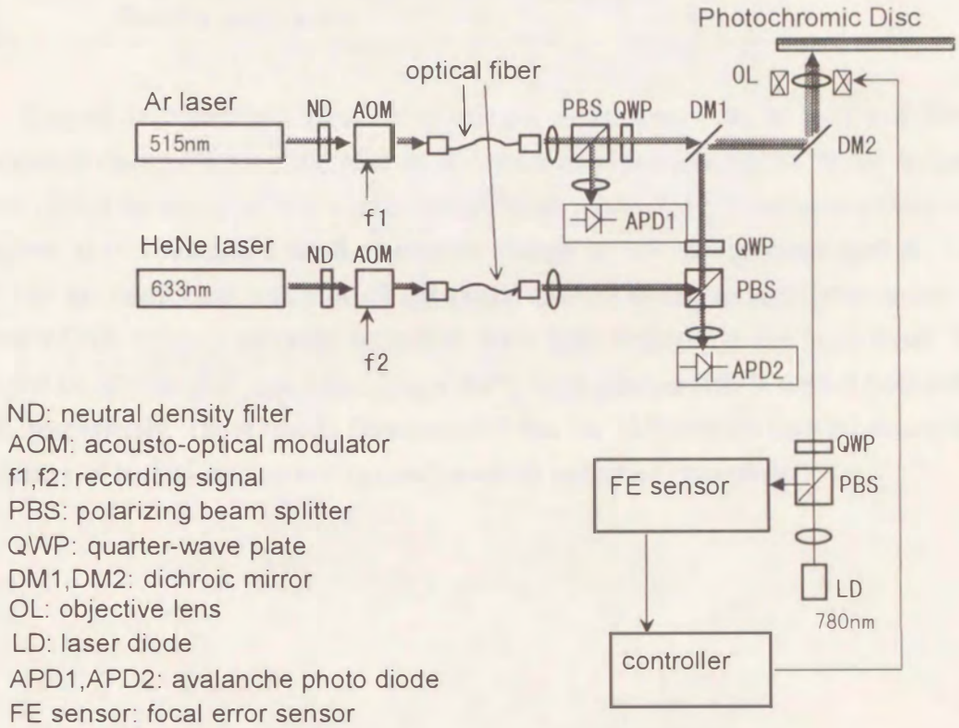

Figure 5-9. The apparatus for SLP two-wavelength recording and readout.

Table 5-III. SLP 2-wavelength write/read conditions

	CH1	CH2
Laser wavelength (nm)	515	633
Writing power (mW)	2.0	1.7
Reading power (nW)	30	20
Recording signal frequency (kHz)	240	300
Relative speed (m/s)	1.4	

Figures 5-10 and 5-11 show the output power spectra of the Ar laser and HeNe laser readout channels before and after the crosstalk reduction operations. In the Ar laser channel (CH1) the crosstalk was a considerably small value of -30 dB reflecting the lower absorption at 633 nm and a small absorption change at 515 nm for compound A. The CNR was an insufficient value of 40 dB (RBW10kHz) owing to high laser noise; an improved CNR value is expected for a low noise light source. On the other hand, the CNR and crosstalks after operations in the HeNe laser channel (CH2) were 50 dB and -40 dB, respectively. These results demonstrated that the SLP readout method allows the coexistence of multiplexed recordings and crosstalk reduction operations.

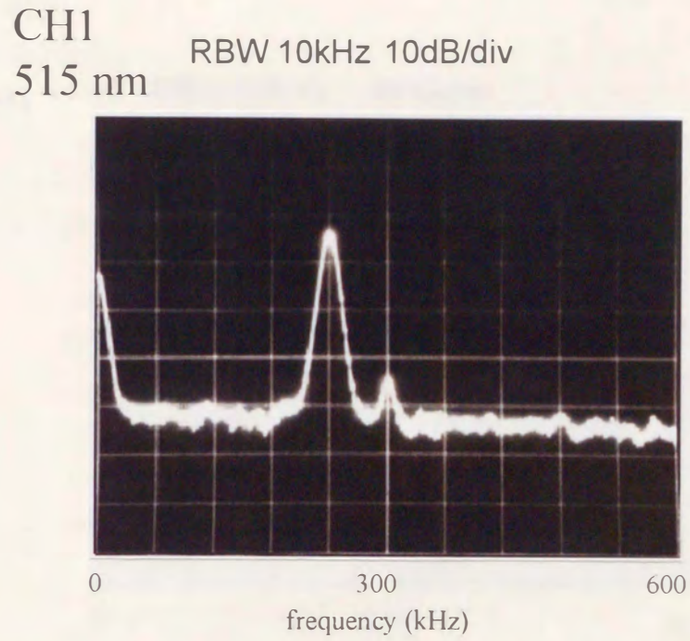

Figure 5-10. Output power spectra of Ar laser readout channel (CH1) before crosstalk reduction operations

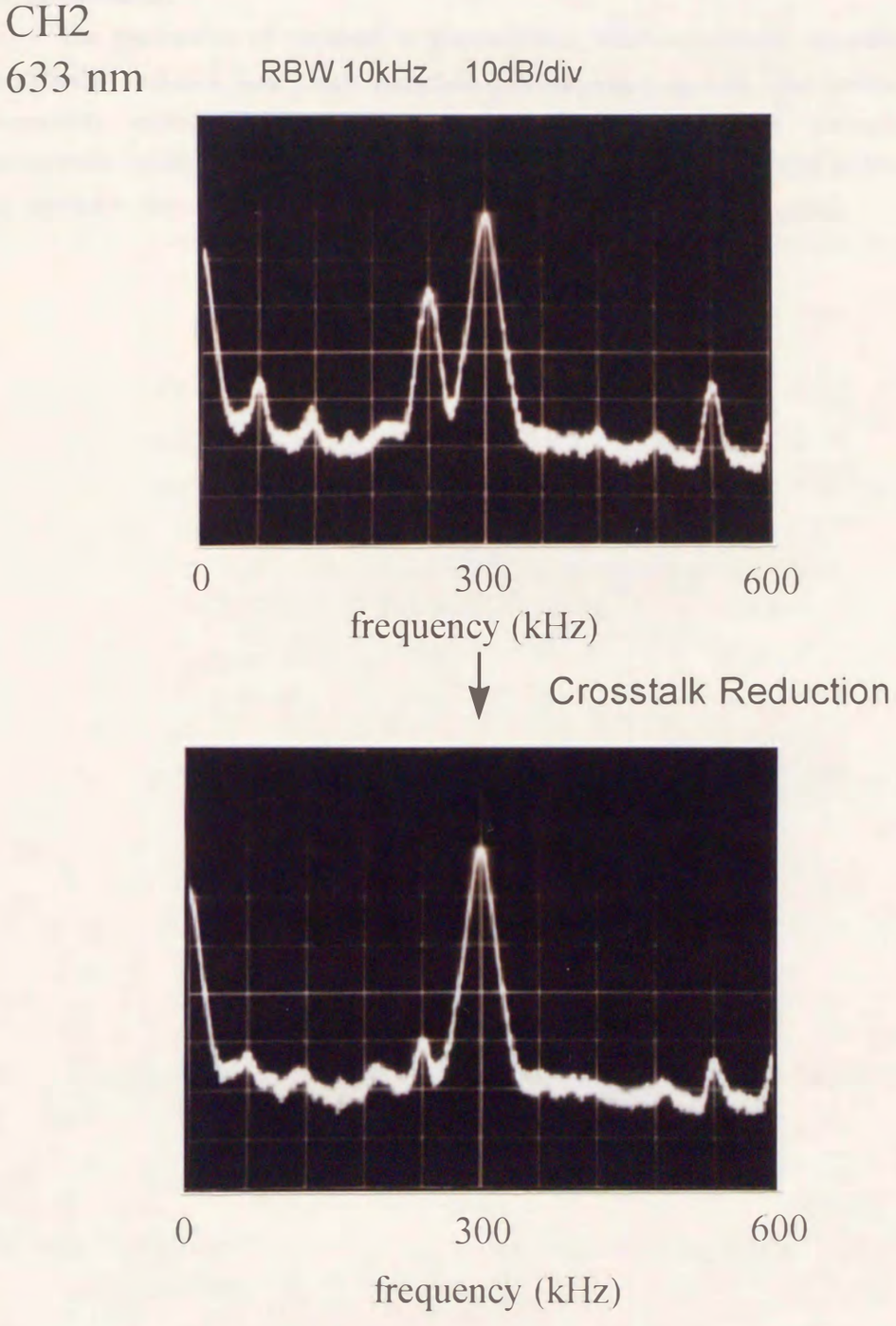

Figure 5-11. Output power spectra of HeNe laser readout channel (CH2) before and after crosstalk reduction operations.

5.6 Conclusion

The mechanism of crosstalk in photochromic multi-wavelength recording was theoretically analyzed, and a new reduction method was proposed. This method was successfully applied to two-wavelength optical recording using photochromic diarylethenes having broad absorption bands. The superlow-power readout method was also applied to two-wavelength recording with the crosstalk reduction method.